KfK 3436
November 1982

Isothermal Steam Oxidation of the Ferritic 11 % Cr Steel (DIN No. 1.4914) at 900 to 1300°C

Z. Zurek

Institut für Material- und Festkörperforschung
Projekt Nukleare Sicherheit

Kernforschungszentrum Karlsruhe

Kernforschungszentrum Karlsruhe
Institut für Material- und Festkörperforschung
Projekt Nukleare Sicherheit

KfK 3436

Isothermal Steam Oxidation of the Ferritic 11% Cr Steel (DIN No. 1.4914) at 900 to 1300 ^{o}C

Zbigniew Zurek

Kernforschungszentrum Karlsruhe GmbH, Karlsruhe

Kernforschungszentrum Karlsruhe GmbH
ISSN 0303-4003

Isothermal Steam Oxidation of the Ferritic 11% Cr Steel (DIN No.1.4914) at 900 to 1300 °C

Abstract

The steam oxidation of ferritic 11% Cr steel tube and sheet samples at 900 to 1300 °C has been studied gravimetrically, metallographically, by X-ray diffraction and in detail by electron probe microanalysis.

The reaction rate could be described by parabolic kinetics of mass increase. During the oxidation a three-layer scale was formed on the surface. The inner layer was composed of iron-chromium spinel, the intermediate layer consisted of a mixture wustite and magnetite, the very thin outer layer was composed of magnetite. Within the inner scale layer small metallic particles enriched of nickel could be observed.

The scale cohesion was generally poor for tube as well as for sheet material and was improving with oxidation time and temperature. After oxidation Pt-markers indicated the growth of inner and outer layer in relation to the initial metal surface. The sheet material specimens exposed at 1000-1100 °C had blisters on their surfaces. A swelling of about 12-15% was measured for the oxidized tubing.

Isotherme Dampf-Oxidation des ferritischen 11% Cr-Stahls (Werkstoff Nr.1.4914) bei 900 - 1300 °C

Zusammenfassung

Die Wasserdampf-Oxidation von Rohr- und Blechproben des ferritischen 11% Cr-Stahls Werkstoff Nr.1.4914 wurde bei 900 bis 1300 °C unter Anwendung gravimetrischer, metallographischer, röntgendiffraktometrischer und elektronenoptischer Methoden untersucht.

Die Gewichtszunahme des Materials in Abhängigkeit von der Reaktionszeit kann durch parabolische Funktionen beschrieben werden. Die während der Reaktion gebildete Oxidschicht hat 3 Teilschichten, die wie folgt zusammengesetzt sind: die innere Teilschicht besteht aus Eisen-Chrom-Spinell ($FeCr_2O_4$), die mittlere aus einem Wüstit (FeO)-Magnetit (Fe_3O_4)-Gemisch, die dünne äußere Schicht aus Magnetit (Fe_3O_4). In der inneren Teilschicht konnten kleine nickelreiche Metallpartikel identifiziert werden. Nach der Oxidation gaben Pt-Markierungen

die mittlere Lage der Ausgangs-Metalloberfläche in Bezug auf die gebildete innere und äußere Teilschicht zu erkennen. Die Schichtstabilität war im Fall von Rohr- und Blechmaterial anfänglich schlecht, nahm jedoch mit Zeit und Temperatur zu. Das bei 1000-1100 ^{o}C oxidierte Blechmaterial zeigte ein großflächiges Abheben der Oxidhaut von der metallischen Unterlage und Blisterbildung.

Die mit der Totaloxidation des Rohrmaterials einhergehende Zunahme des äußeren und inneren Durchmessers (Schwellen) wurde vermessen. Sie beläuft sich auf jeweils etwa 12-15%.

Content

1. Introduction

Recently, heat resistant martensitic 9-12% chromium steels have received wide attention as alternative materials for application as fuel-element components such as wrappers in the liquid sodium cooled fast breeder reactor /1/. Furthermore, this type of steel is under consideration for advanced pressurized water reactors (FDWR). In this connection the behaviour under accidental conditions, when temperatures may raise to above 1000 ^{o}C, is of great importance.

Whereas the high temperature oxidation resistance of iron-chromium steels in air has been known for a number of years and several investigators have studied in detail the kinetics and mechanism of reaction, an equally important corrosion problem, namely by steam and steam containing atmospheres, has received little attention.

The limited data available for the high temperature reaction of iron-chromium steel in steam, reveal that oxidation of chromium steel like that of pure iron proceeds more rapidly in water vapor than in air /2-4/.

The chemical potential of oxygen in water vapor is many times lower than the oxygen potential in air. Therefore, the chemical and phase composition of scales on the same metallic materials is most frequently different in water vapor atmosphere than in air or oxygen. When metals can form with oxygen several individual compounds different in the degree of metal oxidation, then a heterophasic scale is generally formed in air atmosphere. Instead a single phase scale is formed in water vapor, since higher oxides are thermodynamically unstable in such conditions. Hydrogen is the second corrosive component in steam atmosphere and its penetration into the metallic phase can cause changes in its physical properties /5-7/.

The detailed studies by Fuji and Meussner /8,9/ on oxidation kinetics of chromium steel in an atmosphere of ArH_2O ($p_{H_2O} \leq 0{,}1$ atm) at 700-1100 have shown that the above reaction obeys in principle the paralinear rate law. Namely, at the beginning of oxidation the process proceeds according to a parabolic and is followed by a linear rate law, the transition being gradual.

The above authors found that this scale is composed only of two layers: a porous inner layer containing spinel phase and wustite and a compact outer one composed only of wustite. The outer layer is divided into sublayers.

This division is the result of cooling down to the room temperature. Alloys containing above 20% chromium oxidize slower only in the initial reactions stage when on their surface a protective Cr_2O_3 layer is formed.

Ipatiew and co-worker /10/ have found that in water vapor at 600-1100, on steels up to 16% chromium a three-layer scale is formed. The inner scale layer consists of a mixture of iron-chromium spinel and wustite the intermediate layer consists of pure wustite; the very thin outer layer is composed of magnetite. The oxidation process in this environment proceeds paralinearly or parabolically.

Differences between results of Fuji and Meussner and Ipatiew et al. are probably the consequence of different conditions in their investigations.

The reason of the higher oxidation rate of iron and Fe-Cr alloys in water vapor atmosphere in comparison with that of oxygen and air has not yet been fully explained. Many authors discuss this effect by water vapor influence on the appearance of defects in the crystal lattice of protective Cr_2O_3 layer in high-percentage chromium alloys of iron. However, in the case of low-percentage chromium alloys of iron with some authors /11/ believe that the higher corrosion rate is connected with better scale plasticity owing to which the contact between metallic core and reaction product is fuller. Namely in water vapor atmosphere higher iron oxides of lower plasticity than wustite cannot be formed on the scale surface and as a result, more convenient conditions exist for plastic settlement of scale on metallic core.

This report presents the results of ferritic 11% chromium steel, DIN No. 1.4914 oxidized in flowing steam under isothermal conditions at 900 to 1300 ^{o}C. Two different shapes of material, namely tube and sheet material, were used in the study.

2. Experimental

2.1 Materials

The analysis and treatment of the materials are given as follows:

a) Tube material No. 1.4914, charge B-761

Product of Röchling-Burbach Comp., charge B-761.

The heat treatments consisted of the solution annealing at 1075 ^{o}C/30 min and annealing at 700 ^{o}C/2h. The test specimens were 30 mm long and had an outer diameter of 6 mm and a wall thickness of 0.350 mm.

b) Sheet material No. 1.4914

Product of Röchling-Burbach Comp., charge Ch 51482. The treatments consisted of the solution annealing at 1150 ^{o}C/1h, air cooling and cold deformation $\sim$ 50%. The sheet specimens dimensions were 20 x 50 x 1 mm.

Table 1: Percent Chemical Composition of tube, sheet material and typical chromium steel 1.4914

Material	C	Si	Mn	P	S	Cr
Tube	0.206	0.344	0.298	0.001	0.006	11.48
Sheet	0.172	0.340	0.540	0.005	0.005	10.62
Cr-steel 1.4914	0.120	0.500	1.000	0.030	0.025	11.00

Material	Ni	Nb	Mo	Co	Ti	Cu	Fe
Tube	0.771	0.237	0.602	0.006	0.006	0.024	85.50
Sheet	0.820	0.190	0.490	0.015	-	-	86.81
Cr-steel 1.4914	0.600	0.200	0.600	-	-	-	rest

In fig 1 is shown metallography of unoxidized material.

Prior to the oxidation, the specimens of both shapes were degreased in an ultrasonic cleaner and then the faces of the specimens were electropolished in an electrolyte of 5% perchlonic acid and 95% metanol at about - 20 ^{o}C and 0.03 A/dm^{2} current density.After electropolishing the specimens were rinsed in distilled water and acetone and next dried in a stream of an inert gas.

2.2 Kinetics measurements

The isothermal steam corrosion tests were performed in a nonpressurized laboratory loop (fig 2), consisting of a tubular furnace with quartz evaporater reaction tube, steam condenser, by-pass condenser, temperature recorder and an argon flooding system. The temperature control was performed by a PtRh-Pt thermocouple. Before

running the experiment the specimen was kept in very pure argon for about two hours and then pushed inside the tube into the reaction zone. When the specimen, after about 2-3 min, had attained the furnace temperature the valve was opened for steam inlet. The specimen were then double-sided exposed to slowly flowing steam.

The measurements of the mass increase were carried out, after the reaction, using an analytical balance (type Sartorius - 2004 MPG) with an accuracy of $\pm$ 1 x 10^{-5}g.

2.3 Test performance

During performance of the tests one experimental problem came up. It was concerned with the spalling of the outer layer of oxide scale. This problem was attributed to the specimens which were exposed to high temperatures 900 - 1000 ^{o}C for 2 h, 1100 ^{o}C for 15 min, 1200 for 10 min, 1300 ^{o}C for 2 min.

After the exposure of the specimen in the reaction zone the flow of steam was interrupted by a T-valve. After argon inlet the specimen was pulled out to a lower temperature zone. This rapid thermal shock caused the outer oxide layer to spall.

To overcome this problem within the subsequent tests, the specimen - after admitting argon - was pulled out to a zone of temperature which was 200 to 300 ^{o}C less than the reaction zone and kept there for 5 minutes, and eventually was pulled out of the reaction tube on a large watch glass to prevent any loss of scale.

Any scale, if at all spalling, was collected and weighed to provide the correct weight gain measurement.

2.4 Post-test evaluation metallography, X-ray investigation and marker test

Preparation of authentic undisturbed metallographic sections, particularly from sheet specimens, was a major problem. The scalling specimens were mounted in epoxy custing resin and then were cut into half. Grinding and polishing were carried out with equipment that minimalized edge rounding and chipping of the oxide.

The greatest difficulty was to prepare a specimen with Pt-marker. After many attempts this problem was solved by using, instead of thin wire, a 0.02 mm thick Pt foil and cut into narrow stripe and fixing to the edges of the specimen. The marker study was carried out only for sheet specimens.

X-ray investigations were carried out with selected specimens oxidized at temperatures 1000 ^{o}C and 1300 ^{o}C. For each separate layer powder for the X-ray study was prepared. Only from the inner scale layer it was difficult to prepare powder due to its very good bonding forces. The X-ray investigation of the oxide scale was carried out using a Debye-Scherrer Camera, Siemens K 700.

3. Results

3.1 Oxidation kinetics

The gravimetric results were plotted as square of weight gain per unit area of the original specimen versus exposure time and are presented in table 2 and 3 and figures 3 and 4.

The parabolic realtionship between the weight gain and the oxidation time is indicated with the temperature range of investigation (900 - 1300 ^{o}C): tube and sheet chromium steel oxidation reaction is represented in these plots by linear functions the slopes of which are equal to parabolic rate constants, Kp. The rate constants have been calculated and listed in table 4 for tube and sheet specimens, respectively. In the Arrhenius representations the activation energies of the tube and sheet specimens for the steam oxidation reaction are $\sim$ 47 kcal/mol and 51 kcal/mol, respectively. See figure 5:

$$\text{tube - Kp} = 6.746 \exp\left(\frac{-47{,}229}{RT}\right)$$

$$\text{sheet - Kp} = 7.074 \exp\left(\frac{-51{,}118}{RT}\right)$$

In fig 6 are shown kinetics curves when the weight of oxygen consumed during the oxidation reaction was transformed into weight of reacted metal by multiplying by factor 2.40.

3.2 Metallography

At 900 ^{o}C, 1000 ^{o}C and 1100 ^{o}C, according to the superficial appearance of the outer layer of the scale, formed on both shapes of specimens, was uniform and apparently compact. The adherence was good for longer exposures than 2 hours. On the sheet specimens the surface appearance was light gray with a coarse grain structure whereas tube specimens were light gray, too, but with finer grains. The sheet specimens which were oxidized for a longer time had blisters appearing on the surface during cooling.

The features of the oxidized tube and sheet chromium steel are shown in figures 7 - 19. The investigation of the cross-sections of the cut samples oxidized at 900 ^{o}C, indicated the presence of two layers on the surface of metallic core (fig 7). The samples, oxidized at 1000 ^{o}C and 1100 ^{o}C, revealed a two layers' scale, too. However, the outer layer was divided into two sublayers. Both sublayers were compact (fig 8, 9, 10). The inner layer of the scale was porous, as indicated by the darker patches, but strongly adherent.

In the inner layer the occurrence of small metallic particles was observed which were completely consumed at the boundary of the outer/inner scale layer (fig 11). Microanalysis of metallic particles are presented in table 6.

At 1200 ^{o}C and 1300 ^{o}C the surface of the scale was bluish gray and rough. The roughness of the scale was found to increase with increasing temperature (fig 22). Results obtained in the cross section study were similar to those for the specimens oxidized at the temperatures 900 - 1100 ^{o}C (fig 12 and 13). The compact outer layer consists of white islands in a gray matrix and the thin, white outer sublayer, which appears to be even more compact. These white islands and layer are probably magnetite (fig 14).

After long time oxidation and at high temperature small round voids and cavities begin to form at the interface between the outer and the inner layers of the scale (fig 12 and 13). The number of these voids increases with the consumption of metal and makes the outer scale more porous (fig 15 and 22).

At 900 - 1200 ^{o}C an irregular interface between the metallic and oxidized phase was observed (fig 16, 17), but at 1300 ^{o}C a needle like irregular interface was observed.

The crystal structure of the inner scale formed at this temperature is a columnar one (fig 18).

For comparison cross section study was done for the tube specimens oxidized at 1000 ^{o}C for 6 h, 1100 ^{o}C for 1 h and 1200 ^{o}C 30 min, they possess similar appearance (fig 19).

The metallography study revealed that the ratio of thickness of the outer layer to the inner one does not depend on the time of oxidation but is only dependent on the temperature. The results are presented in table 7 and 8 and fig 20.

The oxidation caused the swelling of the tube specimens. An increase in the outside diameter of 12-15% was measured. The inside diameter decreased by an equal amount.

3.3 X-ray investigation

The X-ray analysis of the scale formed on the chromium steel specimens during steam oxidation showed that the outer layer of the scale which is divided into the two sublayers consist of: The outer sublayer of wustite (FeO) and magnetite (Fe_3O_4), spectra lines of the last one were very distinct. In the inner sublayer FeO and Fe_3O_4 are present but spectra lines of the magnetite were rather weak in this case. The X-ray study of the inner layer of the scale showed it to be the iron-chromium spinel ($FeCr_2O_4$).

3.4 Marker study

The platinum marker placed on the specimen surface before the reaction started was found after the oxidation process at the boundary of the two layers : the inner spinel and the outer wustite layer (fig 21).

4. Discussion

4.1 Oxidation kinetics

In principle, all experimental curves from 900 to 1300 ^{o}C can be expressed as parabolic functions. Such oxidation kinetics denotes that diffusion of reactants in the scale (occurring under time independent concentration differences) is the slowest partial process which determines the rate of formation of the compact product layer.

The curves for sheet and tube specimens in general show similar characteristics for all temperatures. But, after an initial temperature dependent parabolic period of steam oxidation, the parabolic relationship changed to a slow reaction rate as observed for tube specimens. This change is due to the approach towards consumption of the metallic core. Figure 4 shows that the change is observed for run at 1100 ^{o}C, 1200 ^{o}C and 1300 ^{o}C when 70-80% metal was consumed. This change is not abrupt but a gradual one. Behaviour of this portion of the curve is extremely complex. A fairly valid reason appears to be the slow consumption of the remaining metallic core and of existing small metallic particles present in the oxide plus the oxidation of the non-stoichiometric oxide

already formed. After this period only a slight additional weight gain was still observed. It can be explained that metallic core and finally metallic particles were completely consumed and the scale formed on the surface is non-stoichiometric while the oxidation process of the scale still proceeds. During this time the oxidation process obeys parabolic kinetics, too, but oxidation rate is many times lower than the initial one while the metallic core still existed (table 5). The apparent activation energy of 11.5 kcal/mol obtained for the oxidation process when metallic core was consumed is significantly lower than the 29 kcal/mol activation energy reported for iron diffusion in wustite /8/. Low activation energy is probably an average of the processes occurring on sites of different reactivities and phase composition.

The over-all oxidation behavior of the sheet specimens (fig 3) was not observed to deviate from the parabolic reaction law in contrast to the tube specimens. This behavior can be explained by the higher thickness (1.0 mm) of the sheet specimens, since complete metal consumption was not achieved within the investigated time range. These curves correspond to the initial temperature dependent parabolic periods of steam oxidation of the tube specimens.

Similar kinetic curves can be obtained when the weight of oxygen consumed during the oxidation reaction is transformed into weight of reacted metal by multiplying by a factor 2.40, an average value for the AISI 400 stainless steel series /13/. It was assumed that the final stoichiometric oxidation products are formed. The 100% wall consumption was not reached at all temperatures (fig 6). However, complete penetration of metallic core was observed metallographically. While using the calculated factor from the analysis of the 11% Cr steel the theoretical value of 100% wall consumption can be achieved.

A closer look to the experimental results of this work obtained by oxidizing different shapes of ferritic steel in steam indicate that shape of specimens has obviously an influence on the rate of the oxidation. When the process of scale growth proceeds as a result of outward diffusion of metal, the permanent contact between the two solid phases may be ensured only as a result of the plastic flow of scale. The most "convenient" conditions for the plastic deformation of scale exist on flat surfaces. This is why in the course of oxidation of round-shape samples, the scale formed has not, for geometrical reasons, appropriate conditions for plastic deformation. As a result cracks may begin to be formed between the metallic core and reaction product layer and in

consequence the cross section of the path of outward diffusion of metal is smaller. In this connection the rate of oxidation for tube specimens is lower than for that specimen.

Several investigators studying oxidation kinetics are aware that specimen geometry has an influence as oxidation results /15/.Romanski /14/ has shown that, when thick scale is formed, the changing dimensions of the metal specimen are important and, in kinetic studies, allowance must be made for this effect.

The materials inserted into the above mentioned investigation have slight differences in crystal structure and microstructure. However, an influence of the crystal structure on the rate of steam oxidation at range 900 to 1300 ^{o}C seem to be less probable than the shape. At high temperature, due to growth, similarly high grain size for the tube and sheet materials was observed, whereas the difference in the oxidation rate of the tube and sheet was just observed at high temperatures.

Obtained results of this work are in partial agreement with those of Ipatiew and Fuji, Meussner, who noted that oxidation in water vapor of chromium steels containing 1 to 15% obeys parabolic or paralinear laws. The parabolic rate constant is about four times lower than of the present work and the activation energy is (22.0 $\pm$ 1 kcal/md) lower, too. The differences between the results of Ipatiew, Fuji, Meussner and those presented in this work are probably the consequence of different investigation conditions. Namely, the above mentioned authors' experiments concern the cases where the partial pressure of water vapor in oxidizing environment was low. They used the mixture H_2O-Ar and water vapor partial pressures were 0.1-0.05 atm.

4.2 Metallography

Metallographic examination (in cross-section) of the scales formed on the tube and sheet specimens of the iron-chromium steel revealed that the scales produced in the initial parabolic phase of steam oxidation were duplex in nature, while at 1000 ^{o}C, 1100 ^{o}C, 1200 ^{o}C and 1300 ^{o}C the outer layer was further divided into two sublayers. Both sublayers were compact.

At low temperatures and short time of oxidation, while cooling, the irregular cavities appear, which divide, as it was mentioned above, the outer layer in

two sublayers and tend to grow as does the thickness of scale. The geometrical shape of these cavities suggests that they result from plastic deformation due to the stresses present in the swelling scale.

The simplest way for stresses in the oxide to be relieved is for the oxide film to crack. This is likely to happen with scale which has limited ductility. Such cracking has been observed during isothermal oxidation of iron /14/ where it is known that the higher oxides do not deform significantly.

The outer layer contains some voids, the amount of which increases with the consumption of metal. The voids are formed as a result agglomeration of vacancies due to the existence of obstructions at the boundary between outer and inner scale interface. They impede or make impossible the penetration of vacancies from cation sublattice to the metallic phase or their annihilation at this boundary /16, 17/. These voids can be considered, too, to be associated with the oxidation of FeO to Fe_3O_4 with the consequent reduction in oxide volume /18/.

Metal grains partially surrounded by penetrating oxide, are clearly seen in the metallic core surface (fig 16, 17). At low temperatures the preferential oxidation of grain boundaries takes place. As the temperature of oxidation is raised the irregularity of the metallic core/oxide interface smoothes up, i.e. the bulk and grain boundary oxidation become similar.

The microanalysis of metallic particles revealed that the chemical composition of metallic inclusions is a function of the distance from the metallic core surface. The inclusions display highest concentration of nickel near boundary between the two layers (outer/inner). A detailed description of behaviour of metallic inclusions will be presented in an other paper.

Comparison of the sample in fig 19, which possesses similar metallographic appearance, reveals essential difference in the weight gain. This disagreement between weight gain and penetration of the oxidation is very difficult to discuss in detail. However, it can be consequence with non-stoichiometric oxide formed during oxidation.

4.3 Marker study

Platinum marker is located at the boundary of the two scale layers Marker location inside the scale, was considered to be the proof of the existence of

a two-directional diffusion of the two reactants in the oxidation process of this metal. According to the above concept, the outer scale layer is formed as a result of outward diffusion of iron and electrons while the inner layer by inward transport of oxygen.

5. Conclusions

The following conclusions can be drawn:

1. A parabolic rate law is able to describe the steam oxidation reaction of the 11% Cr steel within the temperature range of 900-1300 ^{o}C.
2. The sheet specimens oxidized at a rate slightly faster than the tube specimens.
3. X-ray studies indicated that the outer layer of the scale consists of wustite and magnetite and the inner layer is iron-chromium spinel.
4. Metallography revealed a duplex layer scale.
5. The adhesion of the outer layer was poor and after long time oxidation increasing porosity was observed.
6. Platinum marker was found to be located after the reaction at the boundary between the outer and the inner scale; this indicated that the formation of the outer layer took place due to outward diffusion of iron and the inner layer as a result of an inward diffusion of oxygen.
7. Owing to swelling of the tube specimens the outer diameter increased up to 12-15%. An equal amount of diameter decrease was observed for the inside of the specimens.

6. Acknowledgements

The author would like to thank Mr.H.v.Berg and Mr.R.Kraft for technical support. Thanks are also due to Mrs.B.Bennek-Kammerichs and Mr.P.Graf for their help during the metallography work. The author is particularly grateful to Dr.S.Leistikow and Mr.G.Schanz for helpful and stimulating discussions during the course of this study. The author is indebted to the Institute of Material and Solid State Research (IMF II) in whose laboratories this work was carried out in the frame of safety studies on advanced PWR material behaviour.

7. References

/1/ K.Anderko
J. Nucl. Mater. 95, 31-43 (1980)

/2/ C.R.Wallwork, A.Z.Hed
Oxidation of Metals, 3, 229(1971)

/3/ D.Caplan, A.Harvey, M.Cohen
Corrosion Science, 3, 161(1963)

/4/ C.A.Stearns, F.J.Kohl, G.C.Frybury
J.Electrochem. Soc. 121, 945(1974)

/5/ C.C.Wood, T.Hodgkiess, D.Whittle
Corrosion Science, 198, 142(1966)

/6/ S.Mrowec, T.Werber
Gas Corrosion of Metals
Technical and Economic Information
Warsow, 1978

/7/ M.Yerian, E.Randell, T.Longo
Corrosion 12, 515 (1956)

/8/ C.Fuji, Meussner
J.Electrochem. Soc. 111, 1215 (1964)

/9/ C.Fuji, Meussner
J.Electrochem. Soc. 110, 1195 (1963)

/10/ V.Ipatiew, M.Morozowa
Ucz. Zap. LGU 175, 88 (1954)

/11/ R.Meussner, C.Birchenall
Corrosion 13, 677 (1957)

/12/ L.Mimmel, R.F.Mehl, C.Birchenall
Trans. AIME, 197, 827 (1953)

/13/ S.Leistikow
Proceedings of the 6th International Conference
on Zirconium in the Nuclear Industry, Vancouver, 1982

/14/ J.Romanski
Corrosion Science, 8, 67, (1968)

/15/ P.Mancock
Proceedings of the AGARD Conference,
Lyngby, Denmark, 10-12 April 1972

/16/ C.Wood, D.Whittle
Corrosion Science 7, 763 (1967)

/17/ P.K.Kofstad, A.Z.Med
Proceedings of the 4th International Congress on
Metallic Corrosion, Houston, Texas (1977)

/18/ C.Wood, J.G.Wright, T.Hodgkiess, D.P.Whittle
Korrosion 23, Weinheim, Verlag Chemie, 1971

Table 2: High Temperature Steam Oxidation of the Sheet Specimens Ferritic Steel Nr. 1.4914 in the Range 900 - 1300 °C

Temperature T /°C/	Time t /h/	Weight gain per unit area $\frac{\Delta m}{g}$ /mg/dm^2/
900	2	1839,35
	3	2155,53
	3	2403,17
	4	2755,26
	4	2692,08
	6	3336,82
	6	2932,16
1000	0,5	1820,82
	0,5	1610,94
	1	2507,53
	1	2696,52
	2	3350,21
	2	3426,23
	2	3954,22
	3	4894,71
	3	5156,43
	5	6136,55
	6	6253,80
	6	6131,34
1100	15 min	2812,24
	15 min	2726,12
	0,5	4086,07
	0,5	4039,85
	1	6056,01
	1	5997,34
	2	8593,27
	2	8370,24
1100	4	12198,46
1100	4	11457,77
1200	15 min	4324,81
	15 min	4854,68
	0,5	7051,54
	0,5	7089,85
	1	10064,40
	1	10846,80
	2	12950,29
1300	2,5 min	3285,16
	2,5 min	2754,14
	5 min	4802,16
	5 min	5303,92
	10 min	6393,29
	15 min	8578,20
	15 min	8273,60
	0,5	12353,52

Table 3: High Temperature Steam Oxidation of the Tube Specimens Ferritic Steel Nr. 1.4914 in the Range 900 - 1300 °C

Temperature T /°C/	Time t /h/	Weight gain per unit area $\frac{\Delta m}{g}$ /mg/dm^2/
900	2	1498,20
	3	1988,83
	3	2161,36
	4	2601,80
	4	2118,56
	6	2790,14
1000	1	2210,20
	2	3343,56
	2	2621,44
	4	3756,19
	4	3005,78
	4	4048,44
	6	3944,37
	6	4350,17
1100	15 min	2194,69
	0,5	3213,24
	0,5	3309,52
	1	4061,06
	1	4326,25
	2	4814,12
	2	4850,61
	4	5377,52
	4	5010,01
	5	5591,18
	5	5214,31
	6	5173,02
	6	5327,63
1200	2,5 min	1426,66
	2,5 min	1345,43
	5 min	2348,19
	5 min	2302,57
	10 min	2942,28
	10 min	3125,14
	20 min	4501,53
	0,5	4971,00
	0,5	5239,98
	1	5417,47
	1	5340,00
	4	5711,25
	4	5801,52
1300	2,5 min	2867,90
	2,5 min	2946,91
	5 min	4745,80
	5 min	4614,06
	10 min	5336,57
	10 min	5607,80
	20 min	5685,71
	20 min	5592,00
	2	5898,28

Table 4: Reaction Rate Constants for Ferritic Steel Nr. 1.4914

Nr.	Temperature (^{o}C)	Tube Specimens Kp $(mg/dm^2)^2/min$	Sheet Specimens Kp $(mg/dm^2)^2 min$
1.	900	$2{,}308 \cdot 10^4$	$2{,}175 \cdot 10^4$
2.	1000	$3{,}790 \cdot 10^4$	$1{,}049 \cdot 10^5$
3.	1100	$2{,}837 \cdot 10^5$	$5{,}877 \cdot 10^5$
4.	1200	$8{,}779 \cdot 10^5$	$1{,}996 \cdot 10^6$
5.	1300	$2{,}865 \cdot 10^6$	$5{,}215 \cdot 10^6$

Table 5: Reaction Rate Constants for Ferritic Steel Nr. 1.4914 Tube when Metallic Core was Consumed

Nr.	Temperature (^{o}C)	Kp $(mg/dm^2)^2 min^{-1}$
1.	1100	$1.75 \cdot 10^4$
2.	1200	$2.28 \cdot 10^4$
3.	1300	$3.00 \cdot 10^4$

Table 6: Microanalysis of Tube Specimens Oxidized at 1300 °C after 2,5 min (in %)

Elements	Position of Analysis (fig 11)					
	A	B	C	D	E	F
Cr	-	2.47	3.85	5.47	7.72	11.12
Ni	0.06	0.12	19.12	11.79	2.83	0.73
Fe	77.56	74.56	75.41	80.77	87.92	86.85
Mn	0.31	0.21	0.14	0.11	0.14	0.28
Mo	0.05	0.07	1.11	1.59	1.13	0.69
Si	-	0.17	0.35	0.26	0.26	0.32
O	Rest	Rest	-	-	-	-
	outer layer		inner layer			metallic core

Table 7: Thickness and Ratio of the Thicknesses of the Outer to the Inner Layer of the Scale Formed During Steam Oxidation of the Tube Specimens of Ferritic Steel Nr. 1.4914

Nr.	Time of Exposure /h/	Temperature /°C/	Inner Layer /mm/	Outer Layer /mm/	Thickness Ratio	
					A	$\bar{A}$
1	2		0,167	0,0977	0,619	
2	4	1000	0,167	0,1045	0,649	0,679
3	6		0,185	0,142	0,770	
4	0,5		0,161	0,120	0,747	
5	1	1100	0,199	0,139	0,700	0,771
6	2		0,216	0,174	0,805	
7	6		0,220	0,184	0,834	
8	2,5 min		0,071	0,065	0,933	
9	5 min		0,098	0,082	0,838	
10	10 min	1200	0,095	0,076	0,800	0,843
11	0,5		0,180	0,137	0,765	
12	4		0,199	0,175	0,883	
13	2,5 min		0,152	0,133	0,875	
14	5 min	1300	0,168	0,168	1,000	0,926
15	15		0,228	0,204	0,894	
16	0,5		0,237	0,221	0,935	

Table 8: Thickness and Ratio of the Thicknesses of the Outer to the Inner Layer of the Scale Formed During Steam Oxidation of the Sheet Specimens of Ferritic Steel No. 1.4914

Nr.	Time of Exposure /h/	Temperature /°C/	Inner Layer /mm/	Outer Layer /mm/	Thickness Ratio A	Thickness Ratio $\bar{A}$
1	4	900	0,095	0,062	0,649	0,645
2	5		0,133	0,086	0,642	
3	0,5	1000	0,086	0,042	0,500	0,720
4	1		0,104	0,083	0,791	
5	2		0,181	0,136	0,754	
6	3		0,190	0,155	0,816	
7	0,5	1100	0,190	0,143	0,742	0,800
8	1		0,284	0,207	0,743	
9	2		0,332	0,280	0,871	
10	4		0,560	0,480	0,870	
11	15 min	1200	0,199	0,169	0,825	0,842
12	0,5		0,323	0,294	0,910	
13	2		0,503	0,395	0,786	
14	5	1300	0,213	0,200	0,970	0,930
15	15 min		0,362	0,350	0,961	
16	0,5		0,564	0,491	0,871	

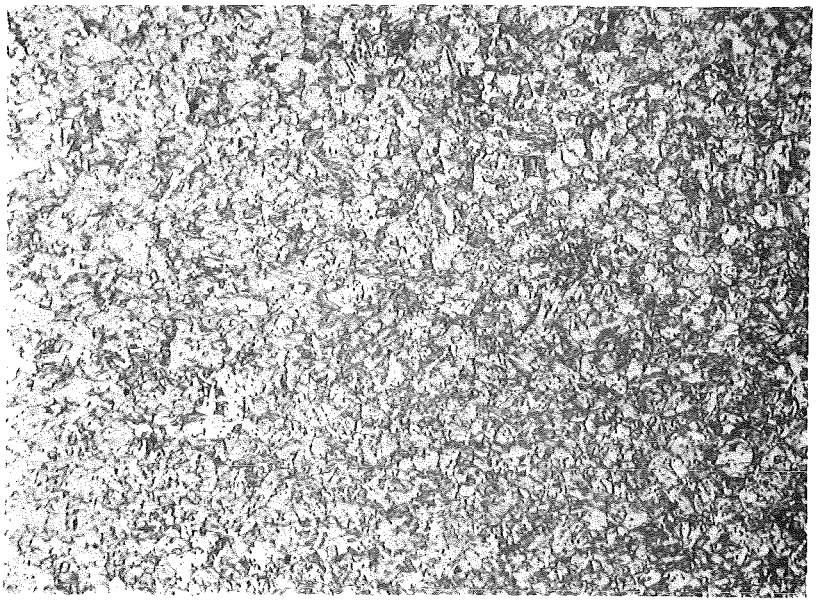

a

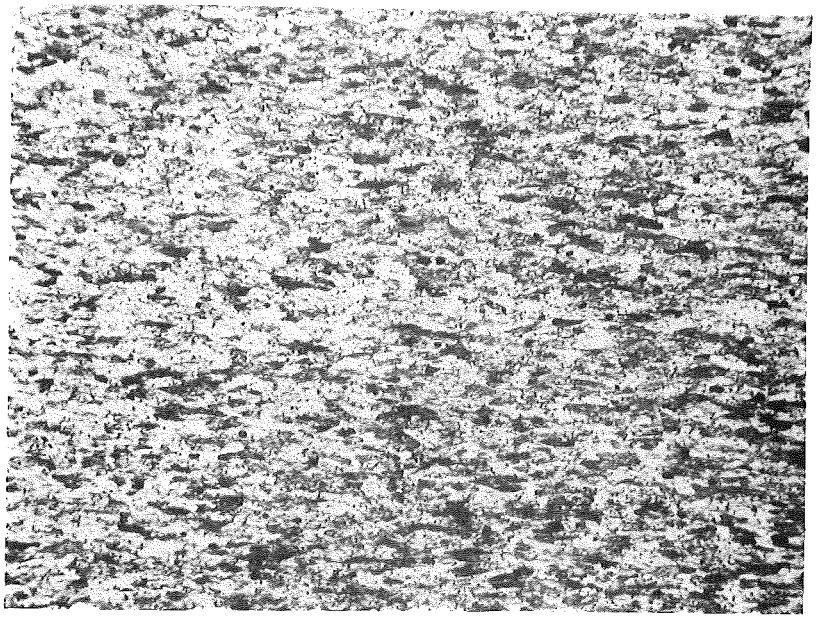

b

Fig.1. Metallography of Unoxidized Material
a) Tube Specimen, b) Sheet Specimen. (X 200)

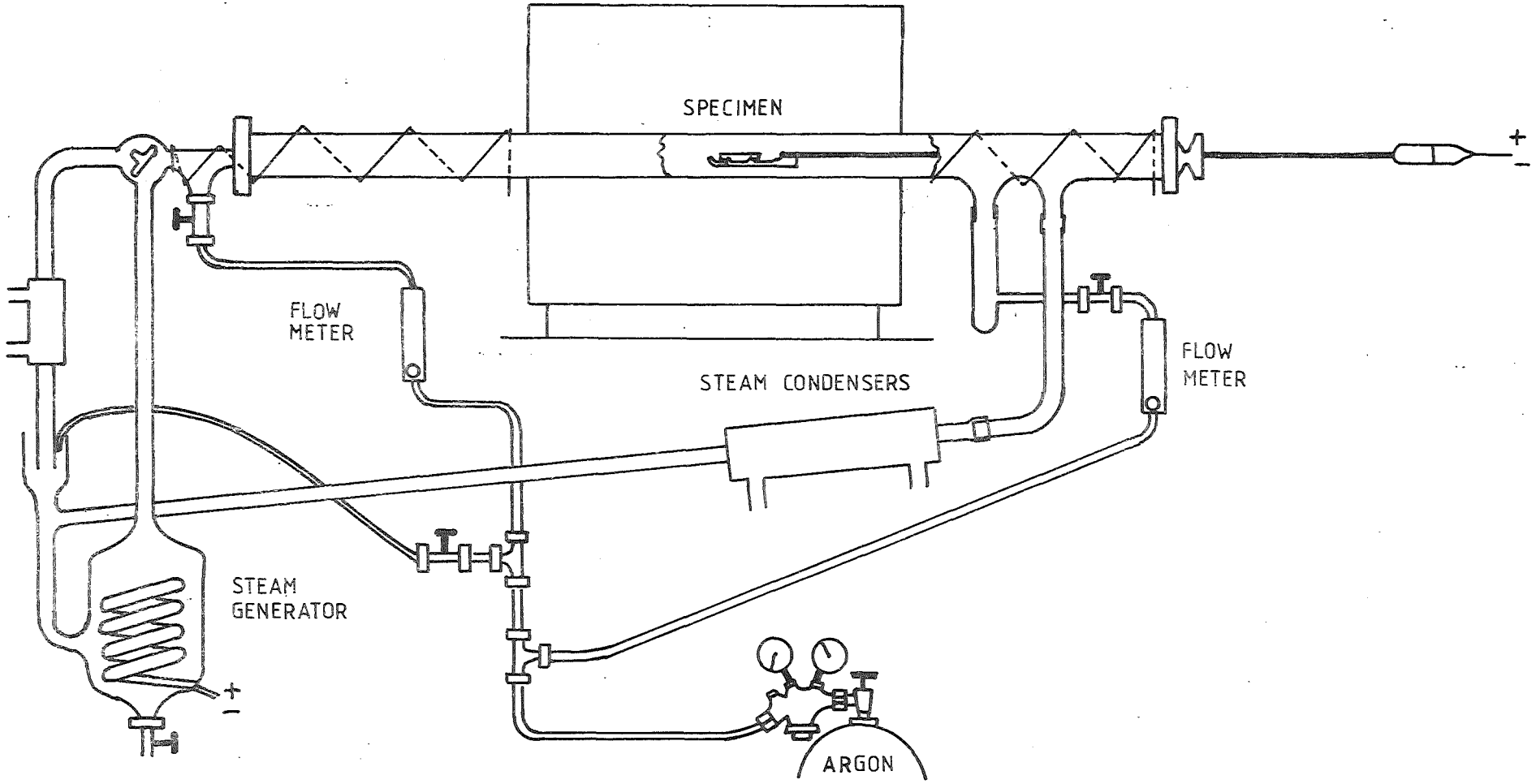

Fig. 2. H.T. - Steam Oxidation Test Equipment

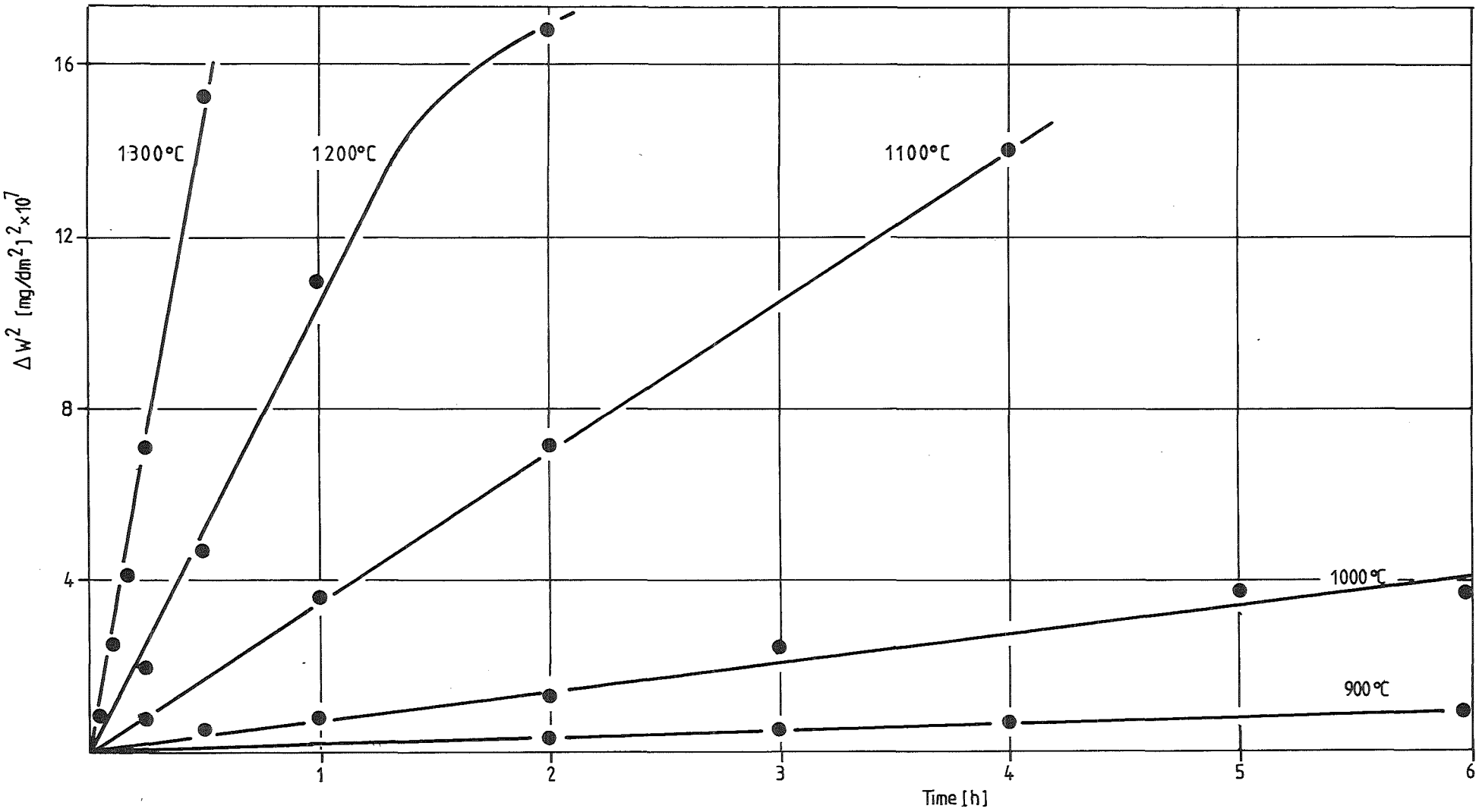

Fig. 3. Parabolic Oxidation of Ferritic Steel No. 1.4914 - Sheet Specimens

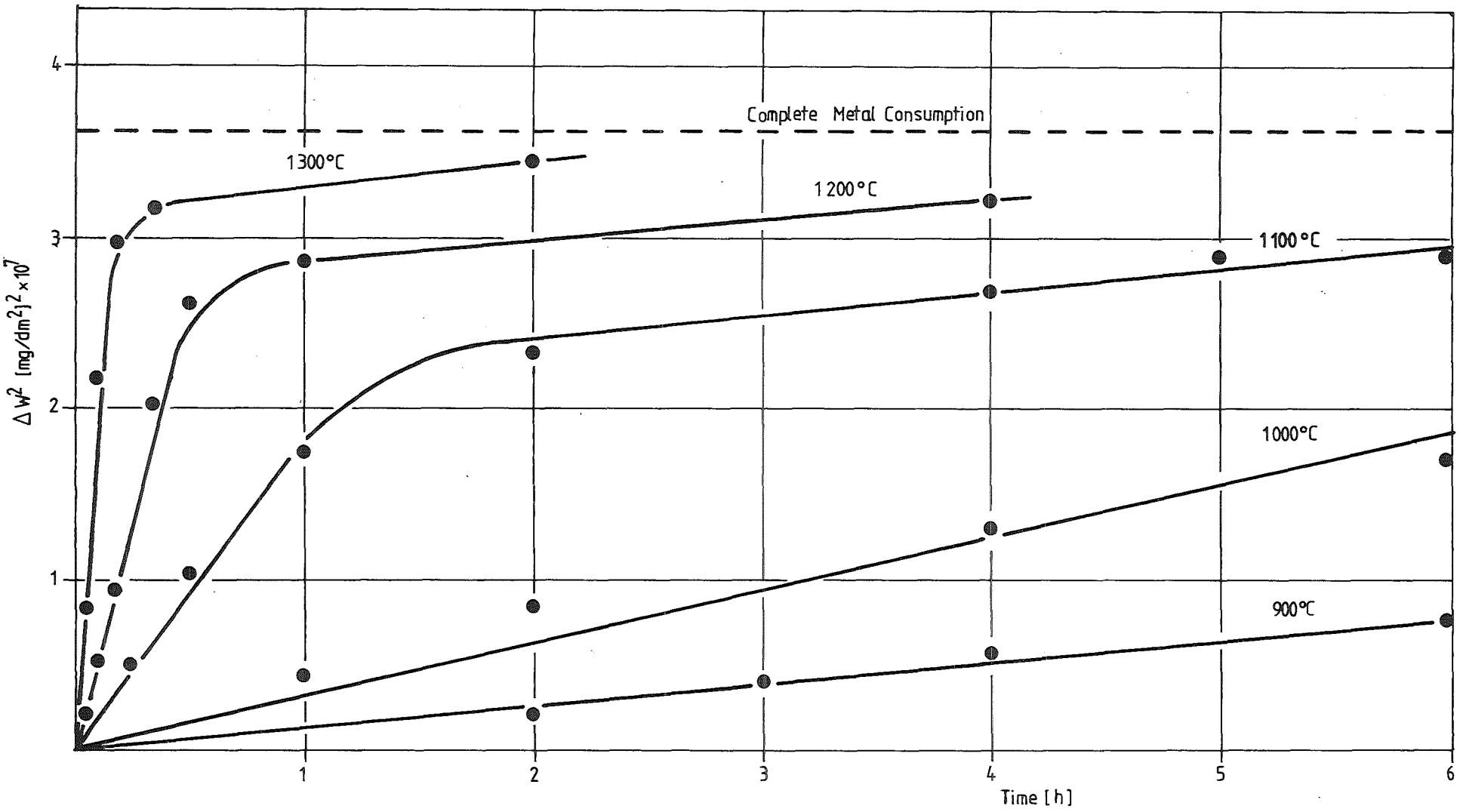

Fig. 4. Parabolic Oxidation of Ferritic Steel No. 1.4914 - Tube Specimens

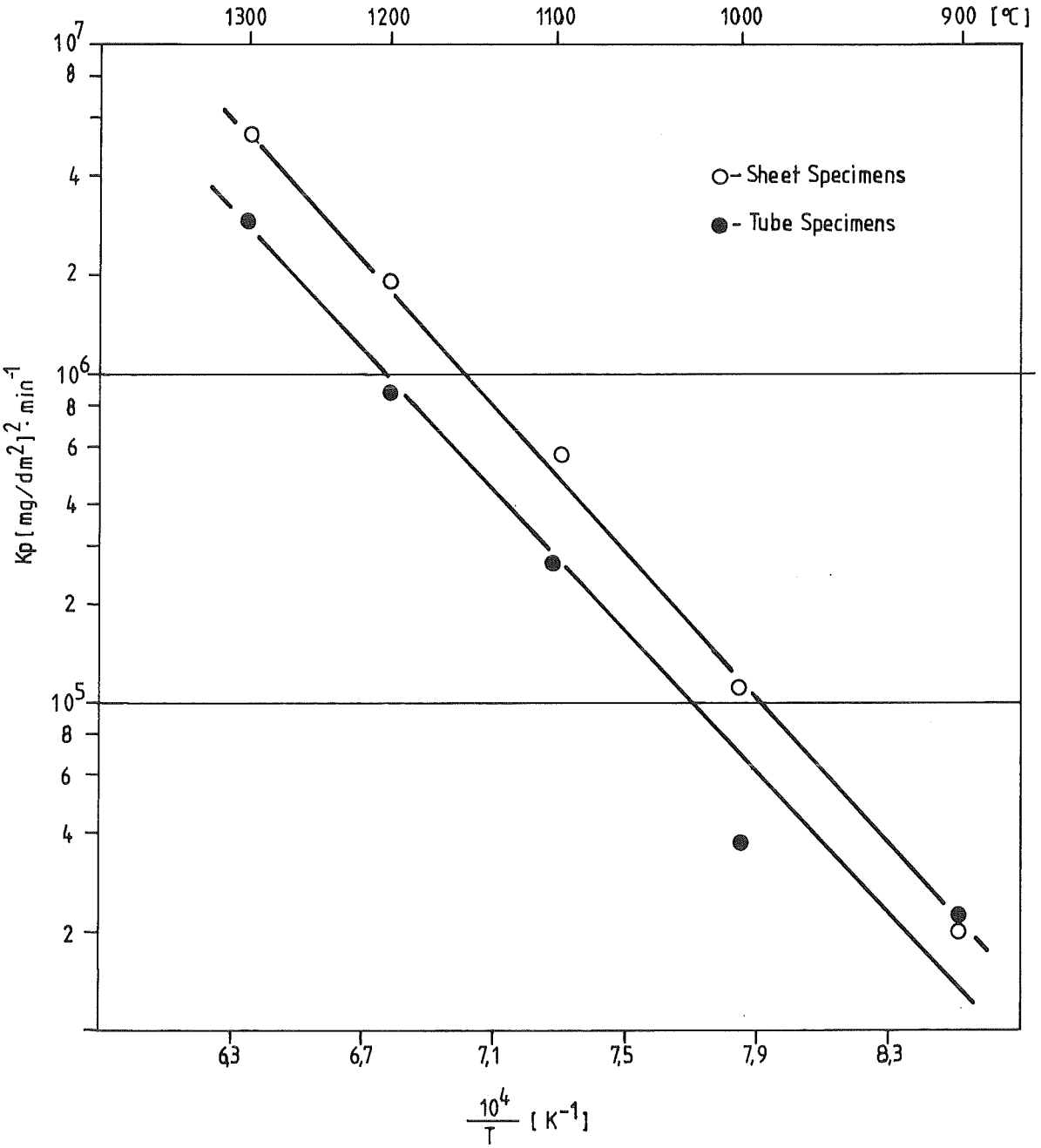

Fig. 5. Temperature Dependence of the Parabolic Oxidation Constant

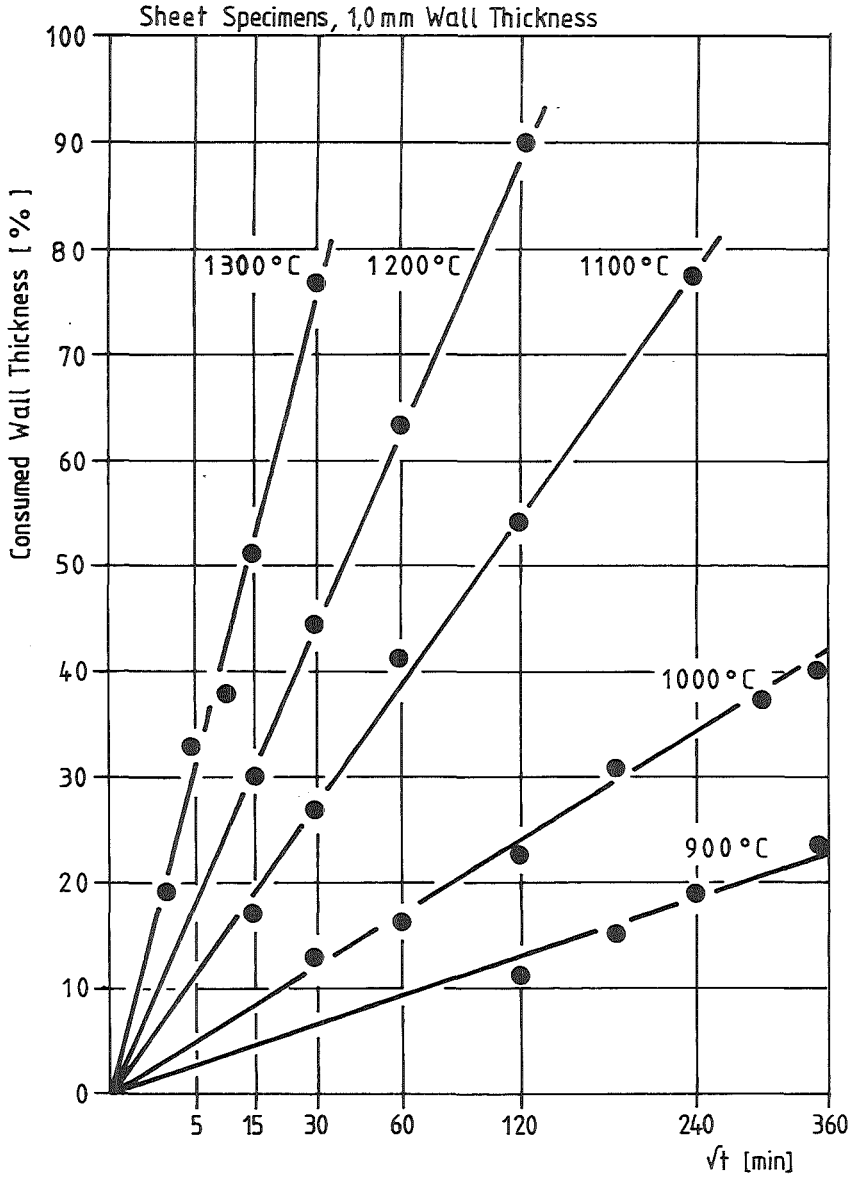

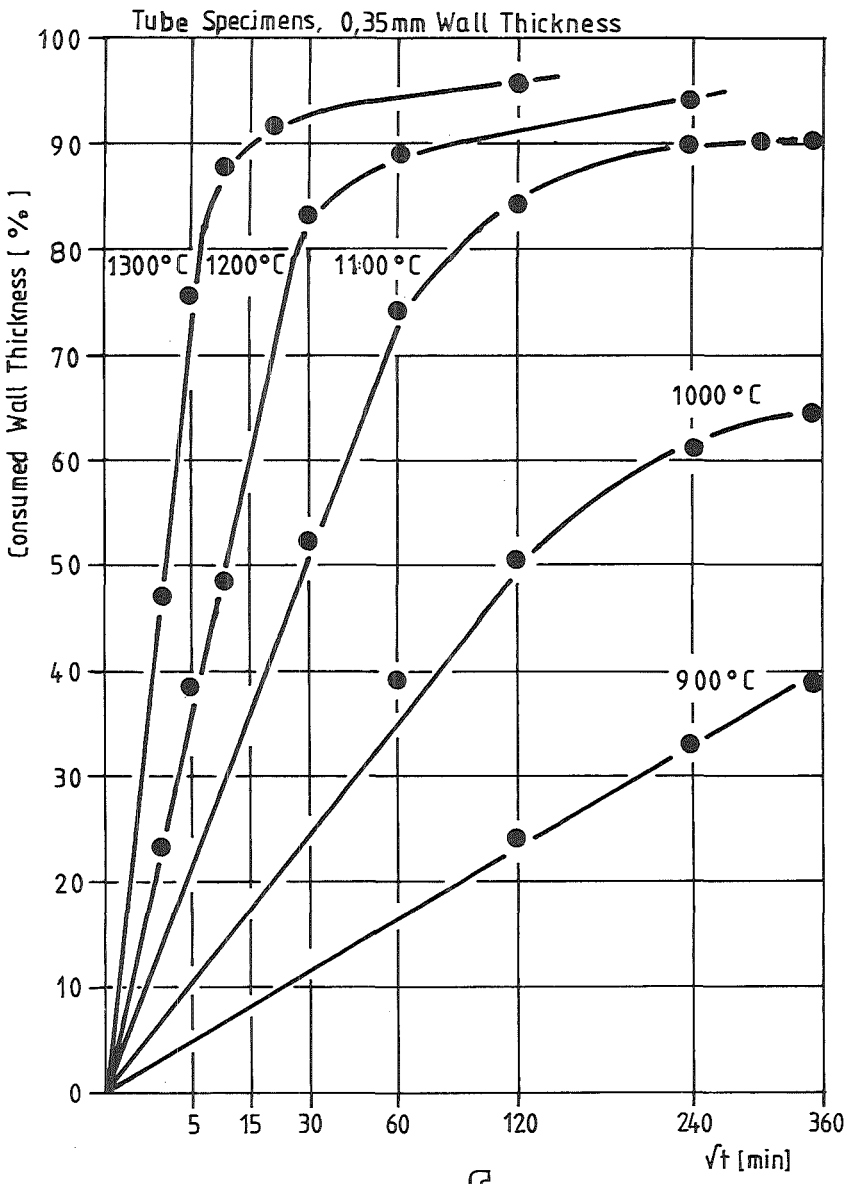

Fig. 6. HT-Steam Oxidation of Ferritic Steel No. 1.4914

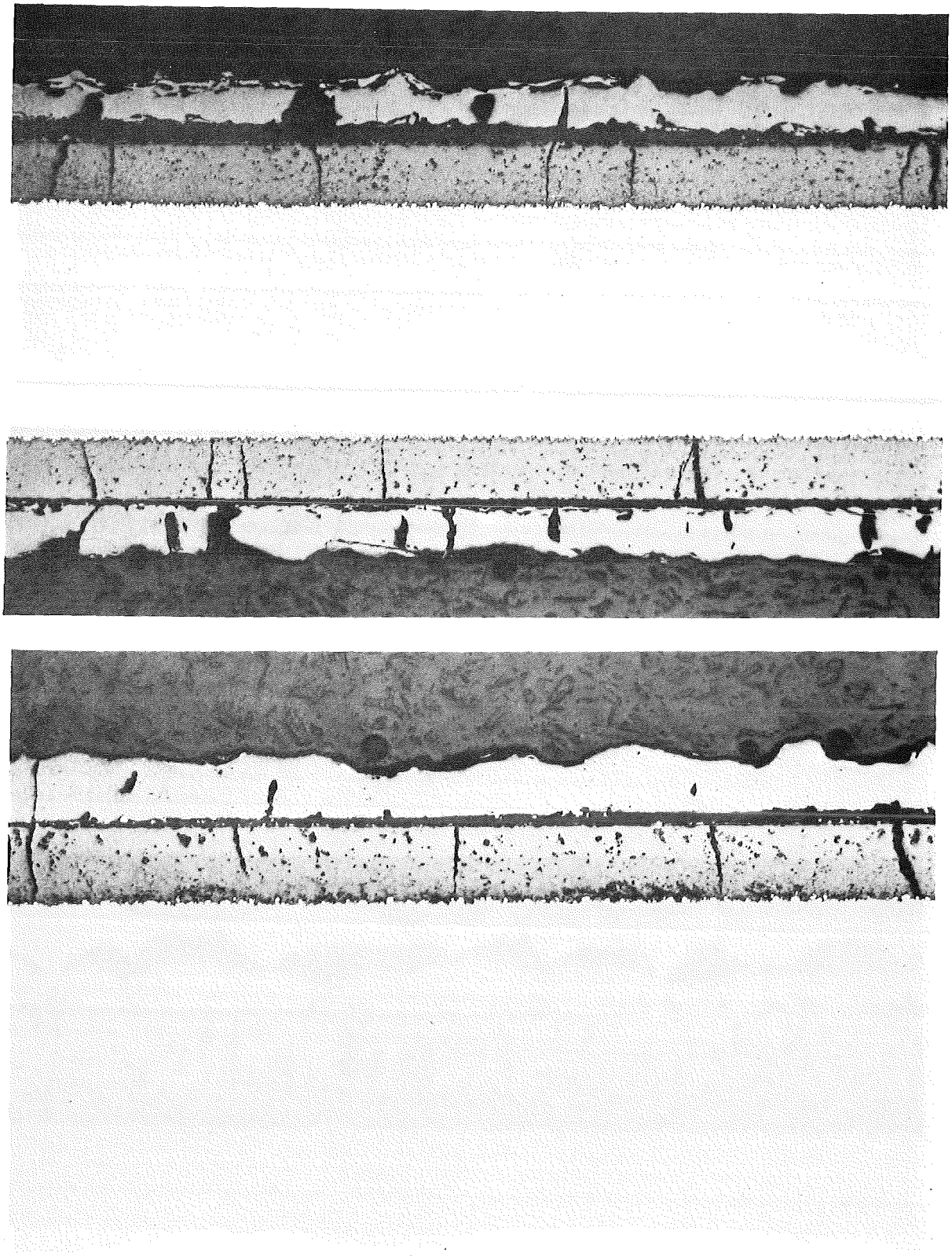

Fig. 7. Ferritic Steel Sheet Specimen Oxidized At 900 °C For a) 4 h And b) 6 h (X100)

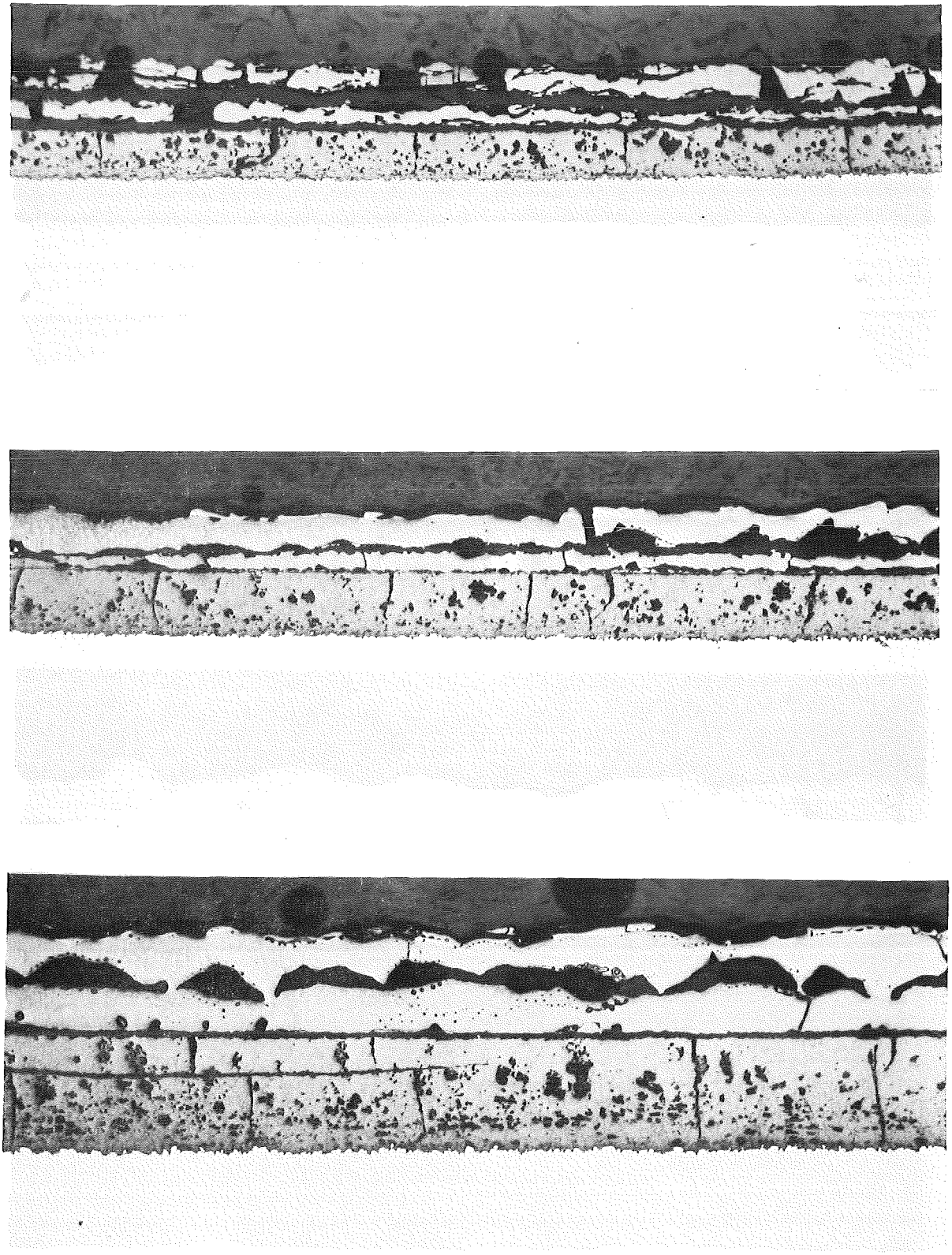

Fig. 8. Ferritic Steel Sheet Specimens Oxidized At 1000 °C For a) 30min, b) 1h, c) 3h. (X100)

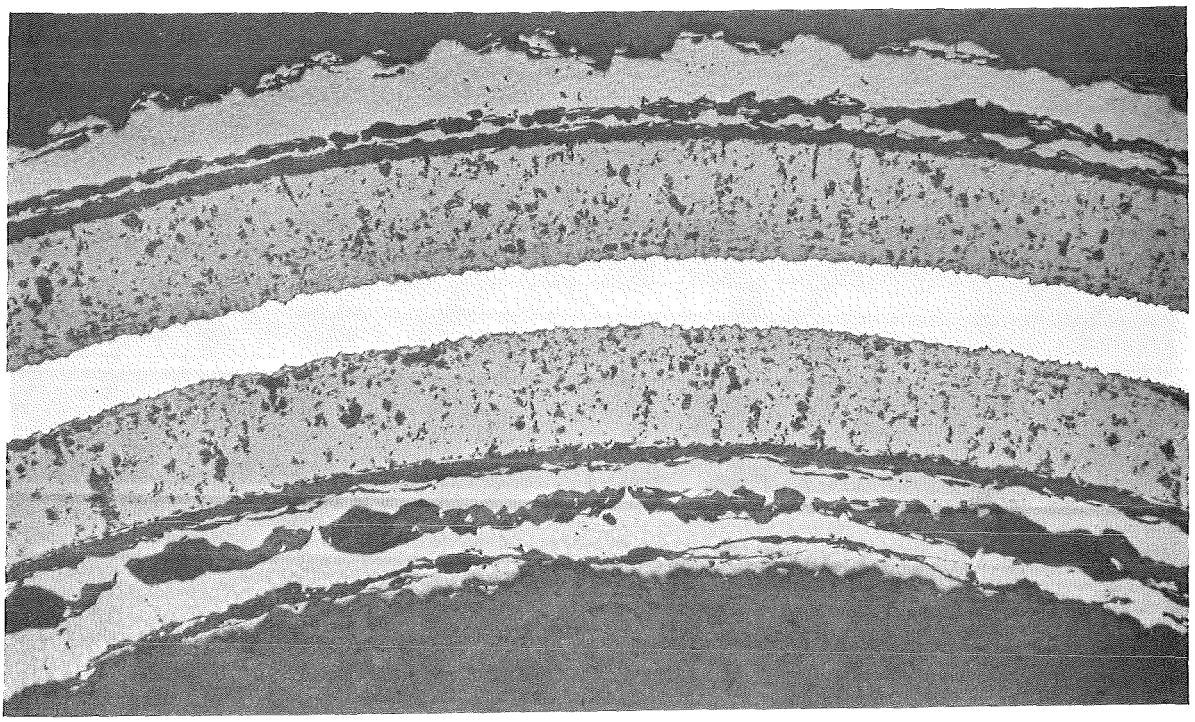

a

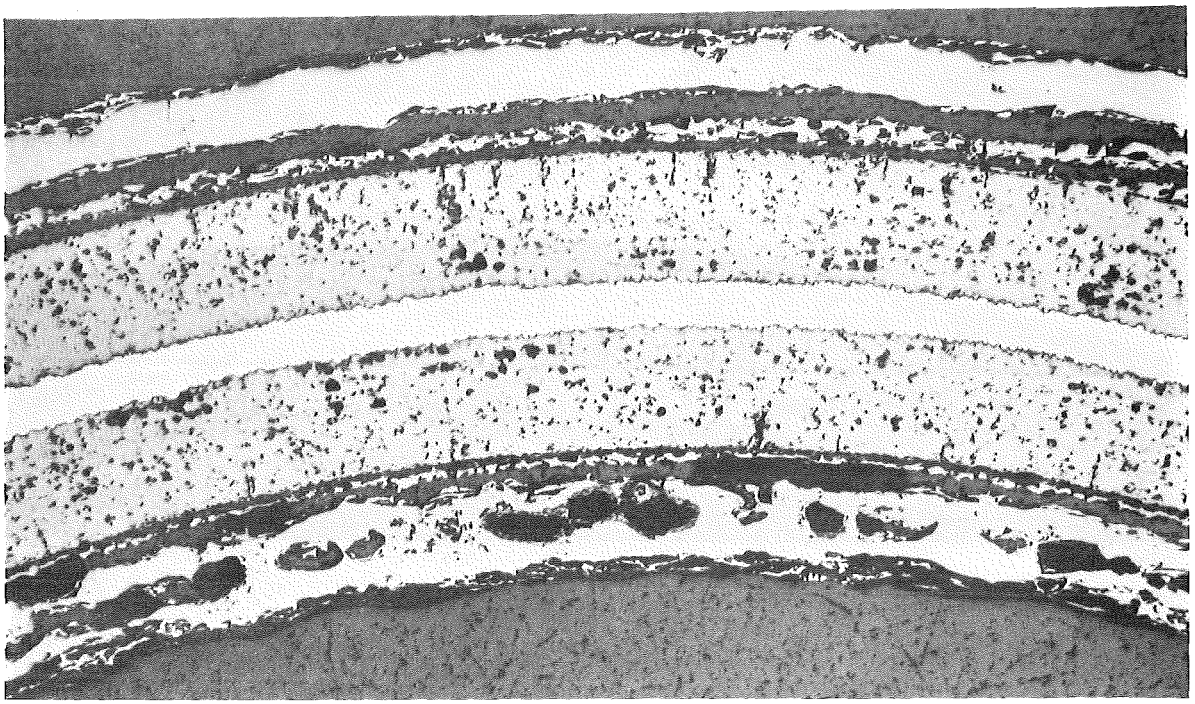

b

Fig. 9. Ferritic Steel Tube Specimens Oxidized At 1000 °C For a) 2 h, b) 4 h. (X100)

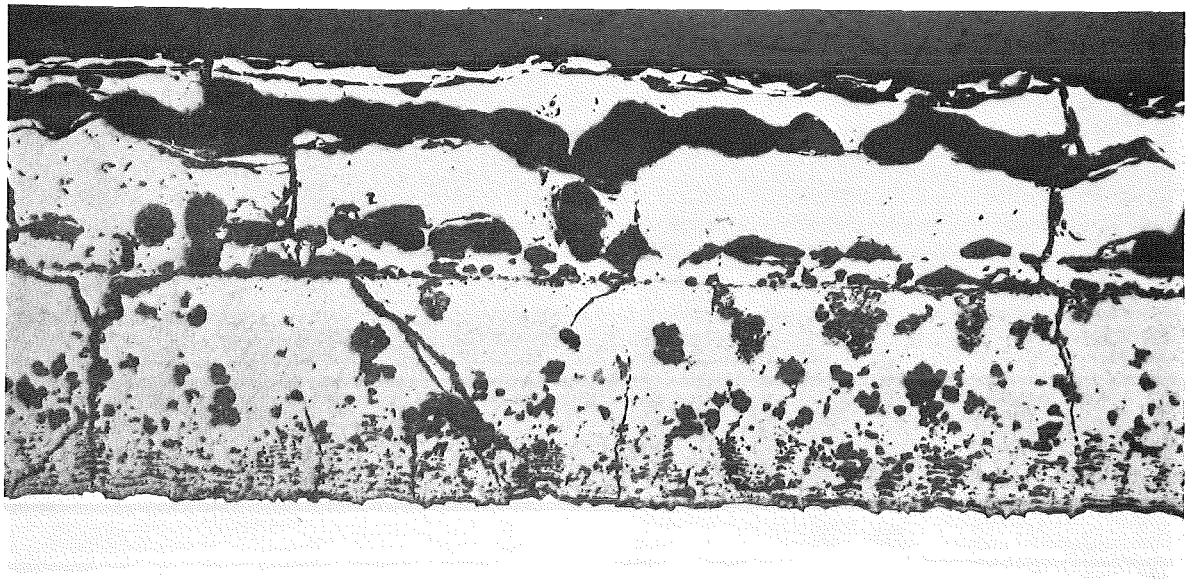

a

X100

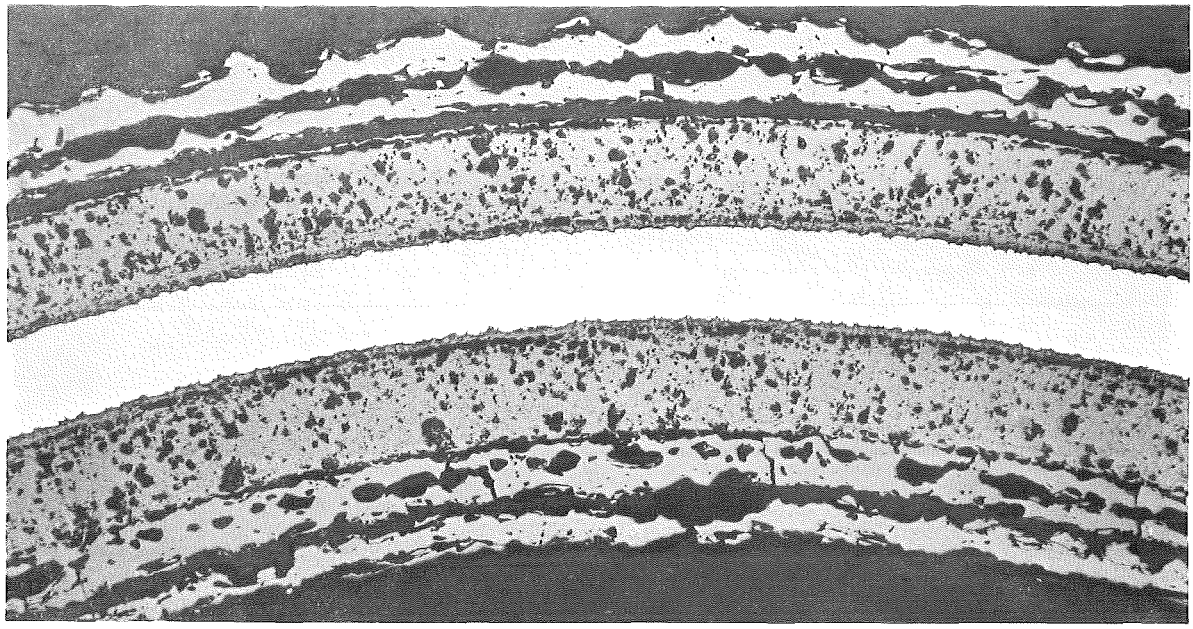

b

X100

Fig.10. a) Sheet Specimen Oxidized At 1100 °C For 2 h.
b) Tube Specimen Oxidized At 1100 °C For 30 min.

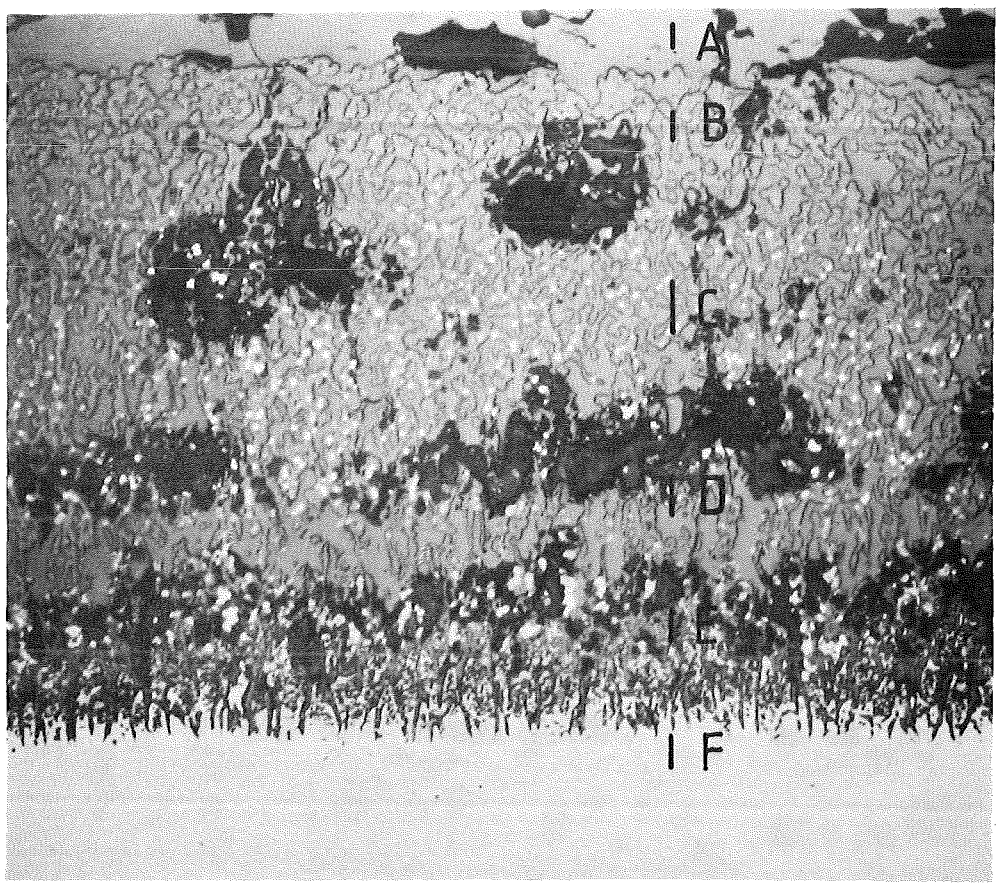

Fig.11. Ferritic Steel Tube Specimen Oxidized At 1300 °C For 2,5 min. (X500)

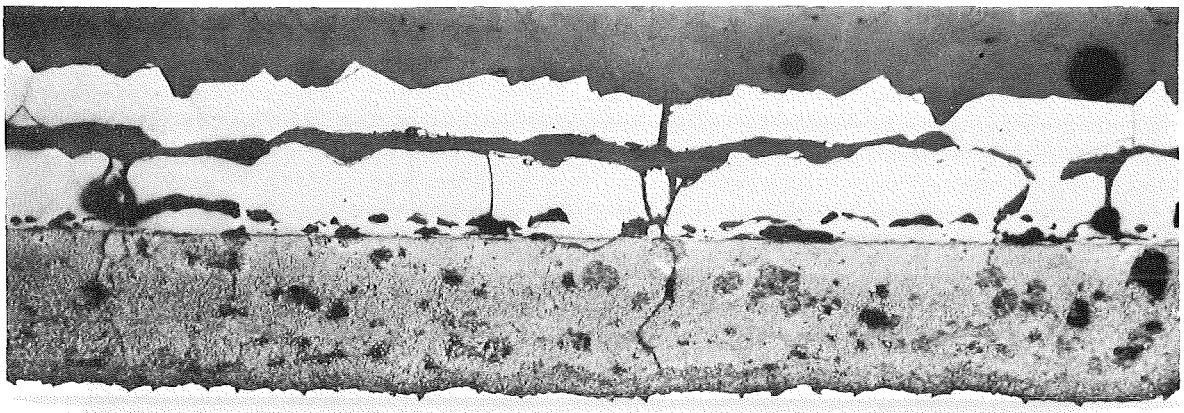

a

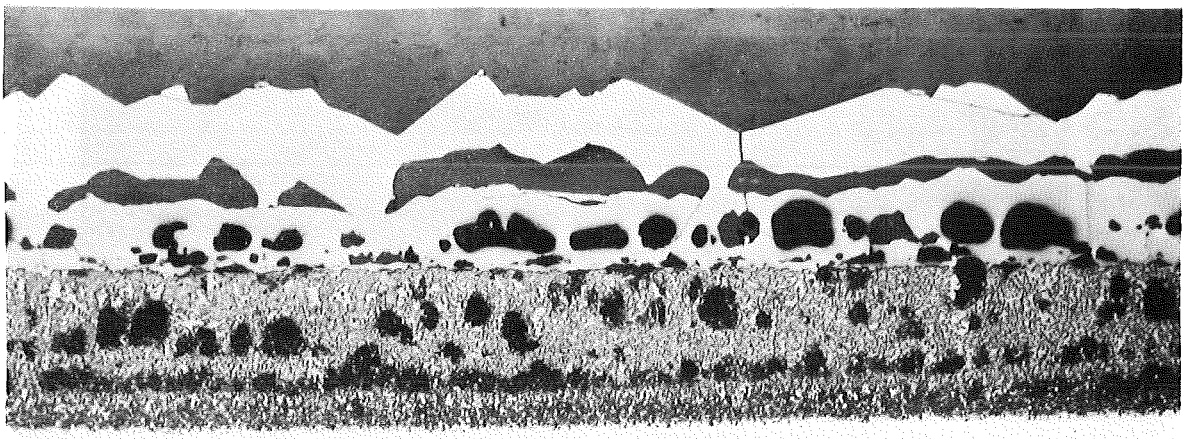

b

Fig.12. Ferritic Steel Sheet Specimen Oxidized
a) At 1200 °C For 15 min, b) At 1300 °C For 5 min.
(X100)

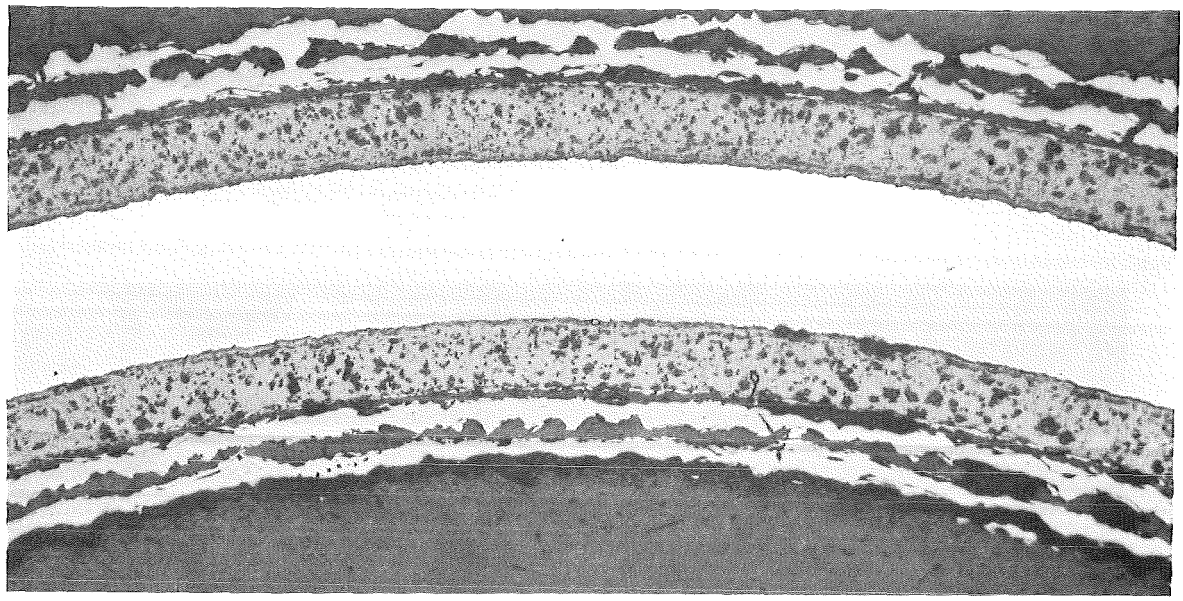

a

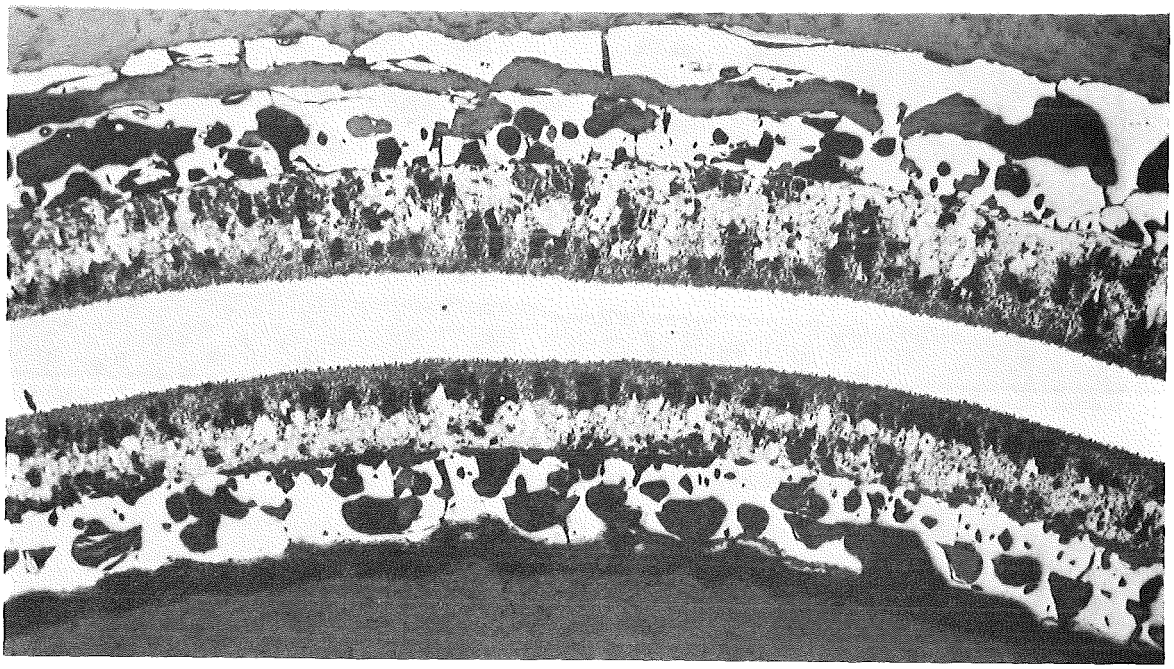

b

Fig.13. Ferritic Steel Tube Specimen Oxidized
a) At 1200 °C For 10 min b) At 1300 °C For 2,5 min
(X100)

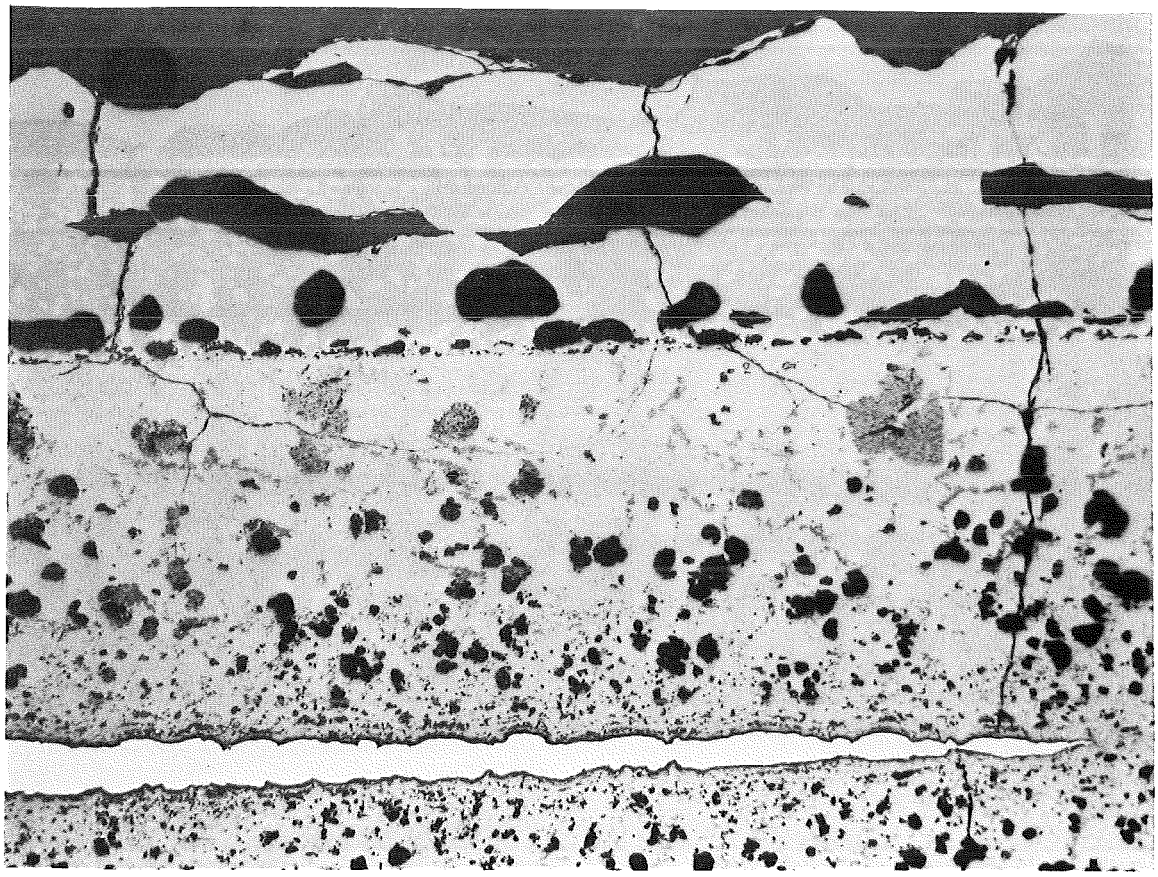

Fig. 14. Ferritic Steel Sheet Specimen Oxidized At 1200 °C For 2 h. (X100)

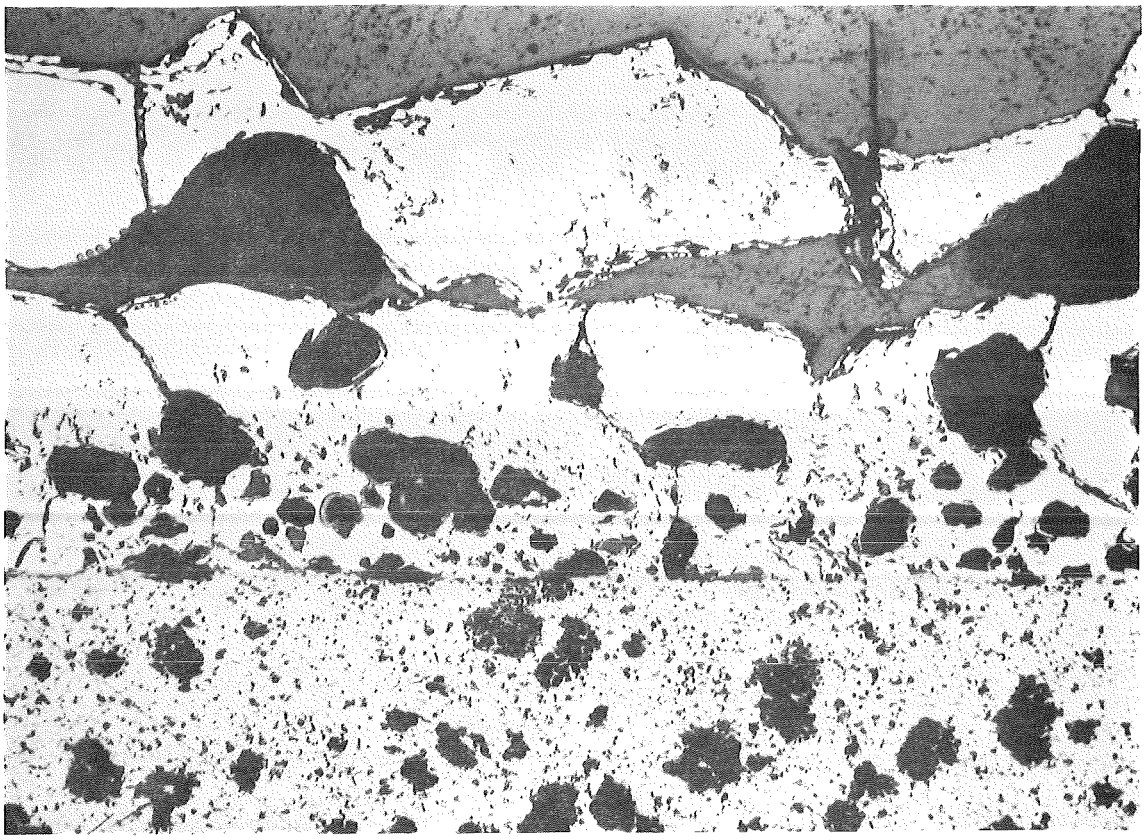

a

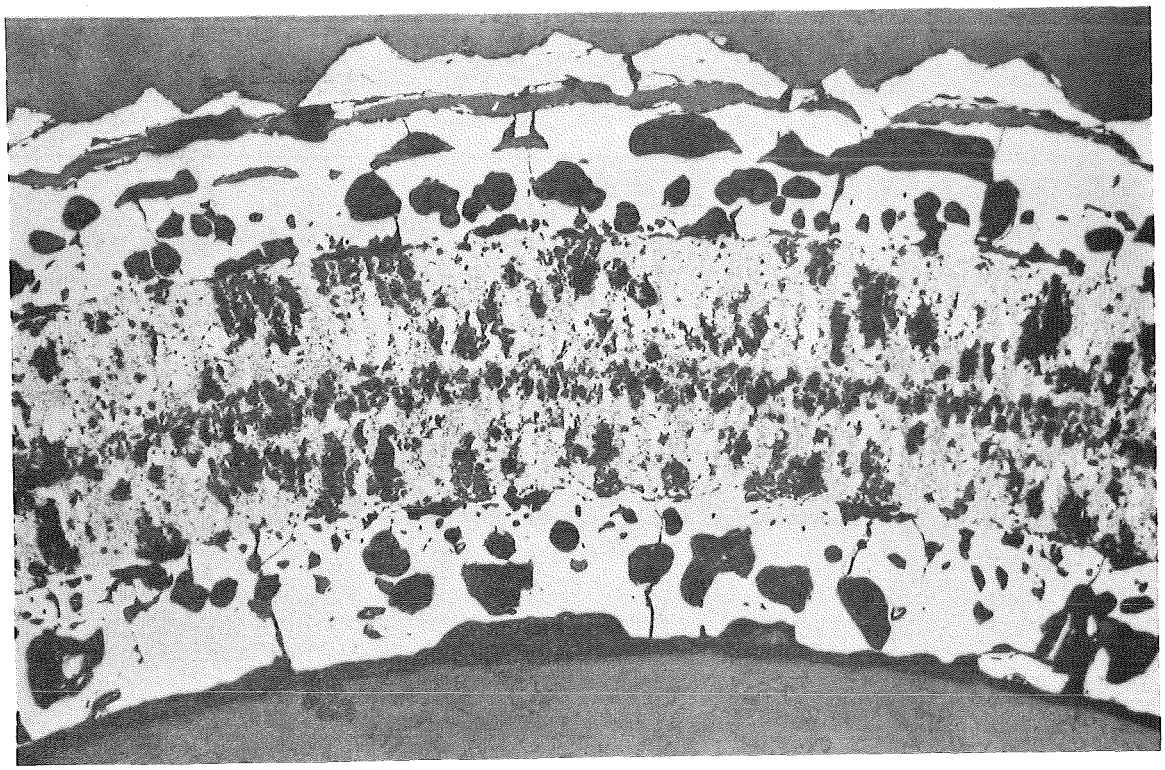

b

Fig. 15. a) Sheet Specimen Oxidized At 1300 °C For 20 min.
b) Tube Specimen Oxidized At 1300 °C For 5 min.
(X100)

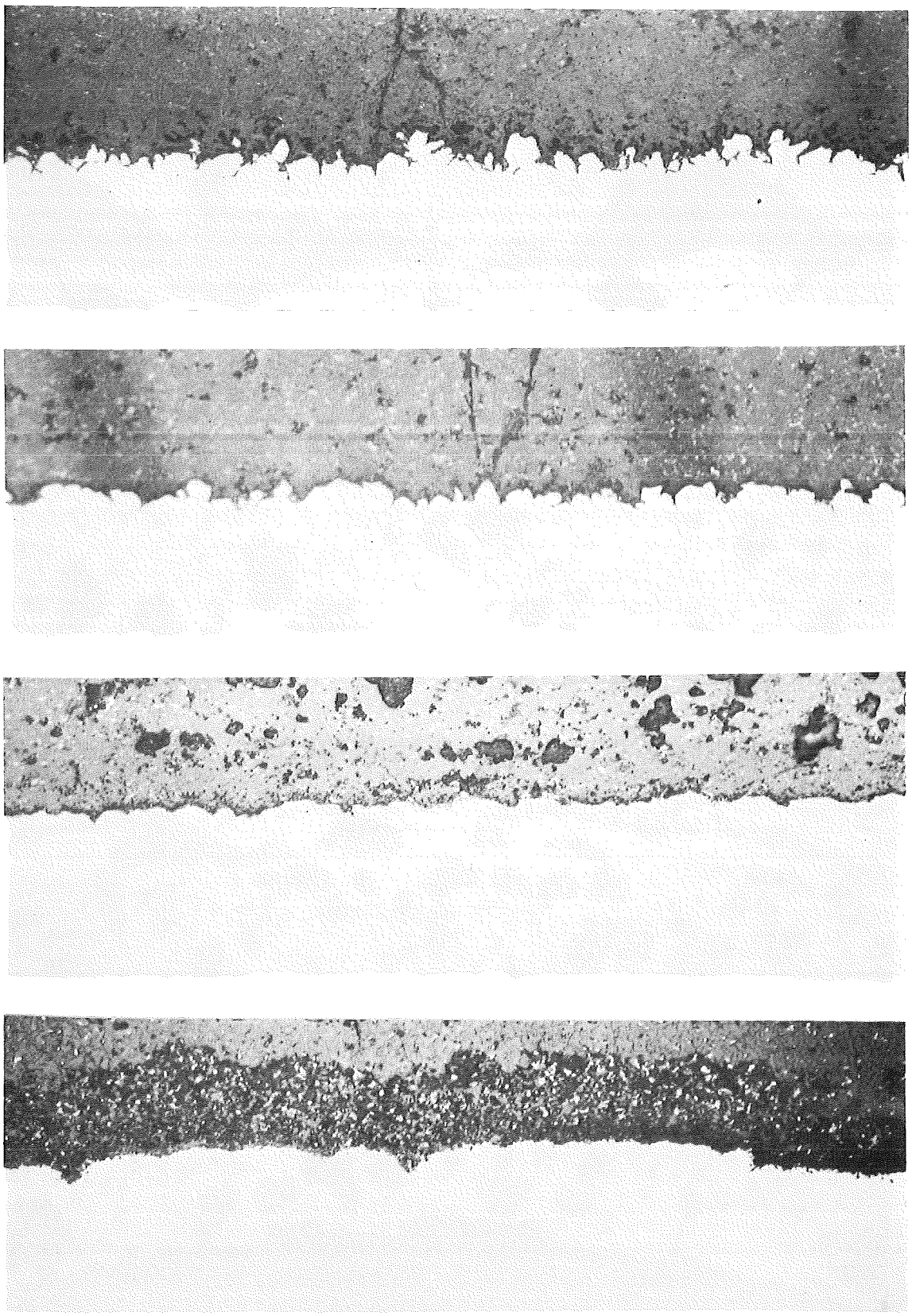

Fig.16. Sheet Specimens Oxidized a) At 900 °C For 6 h, b) At 1000 °C For 1 h, c) At 1100 °C For 30 min, d) At 1200 °C For 30 min. (X 500)

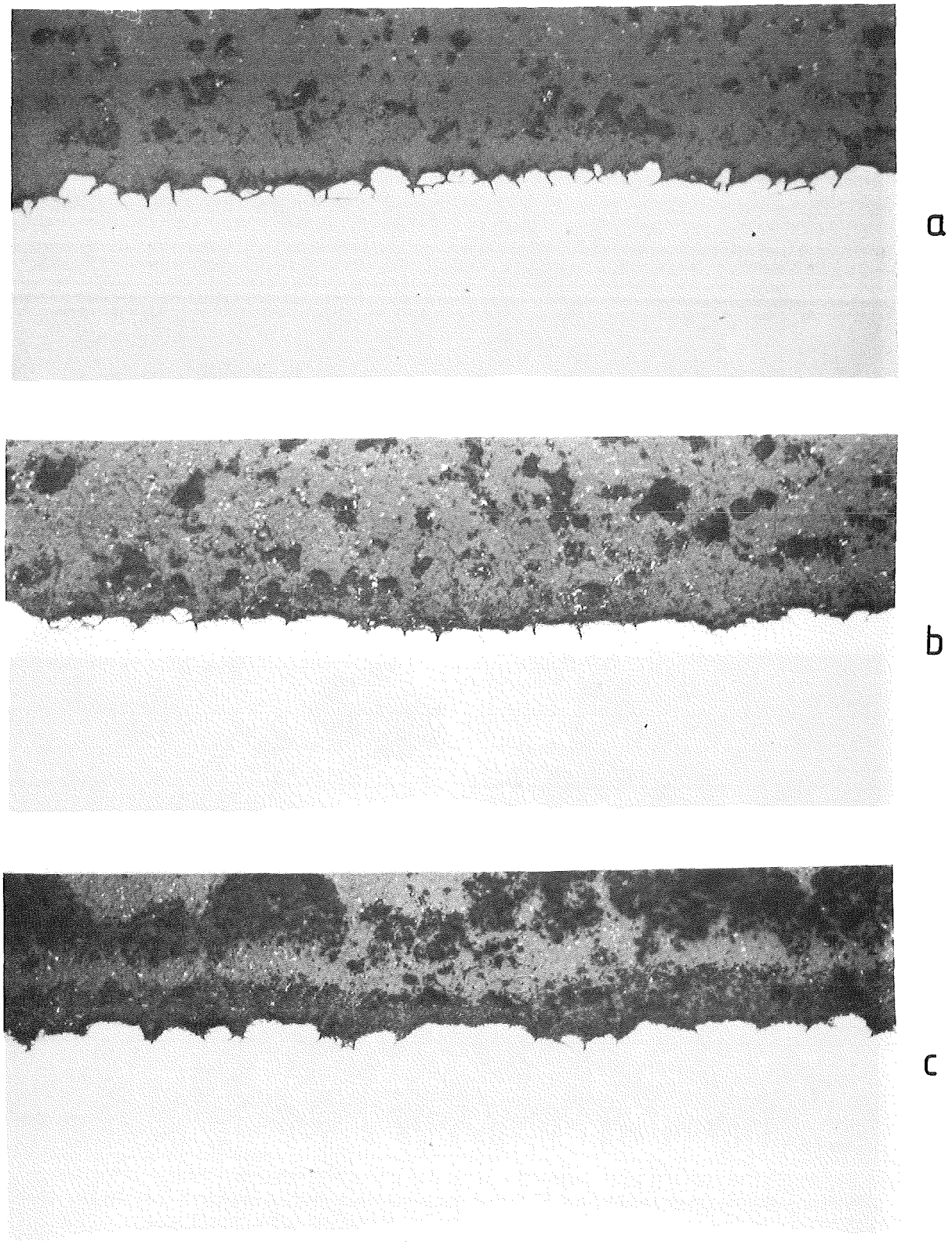

Fig.17. Tube Specimens Oxidized a) At 1000 °C For 2 h
b) At 1100 °C For 30 min, c) At 1200 °C For 5 min.
(X 500)

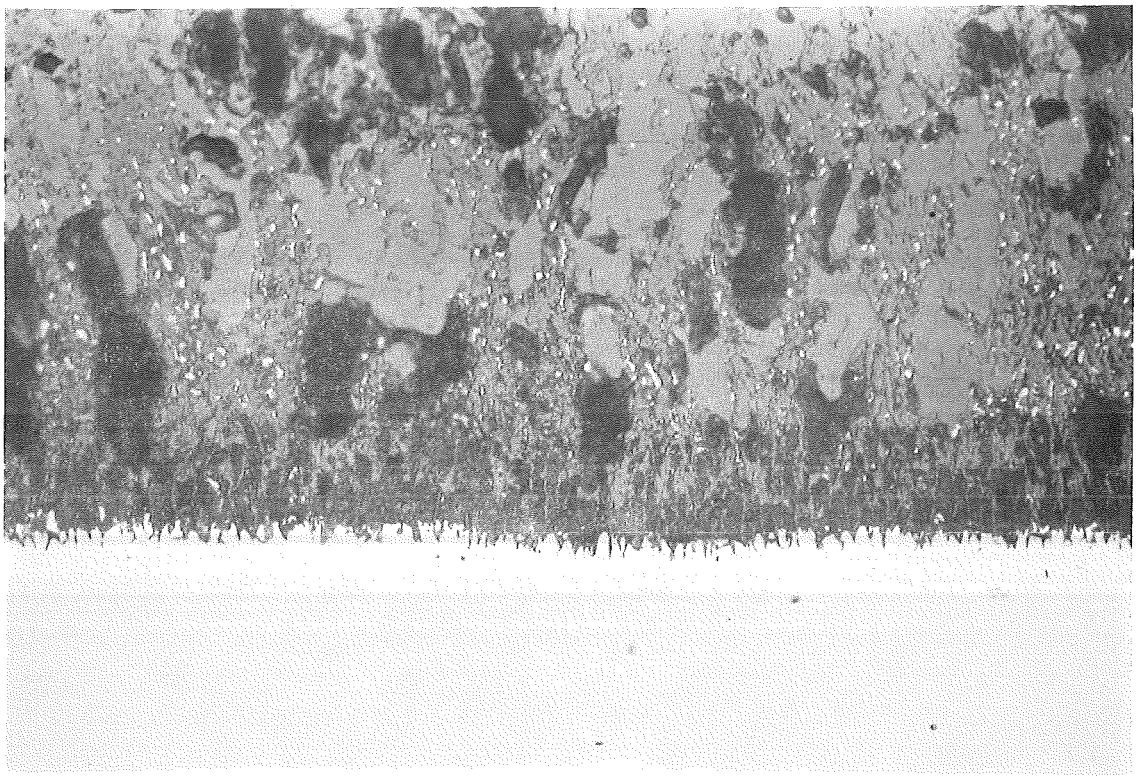

a

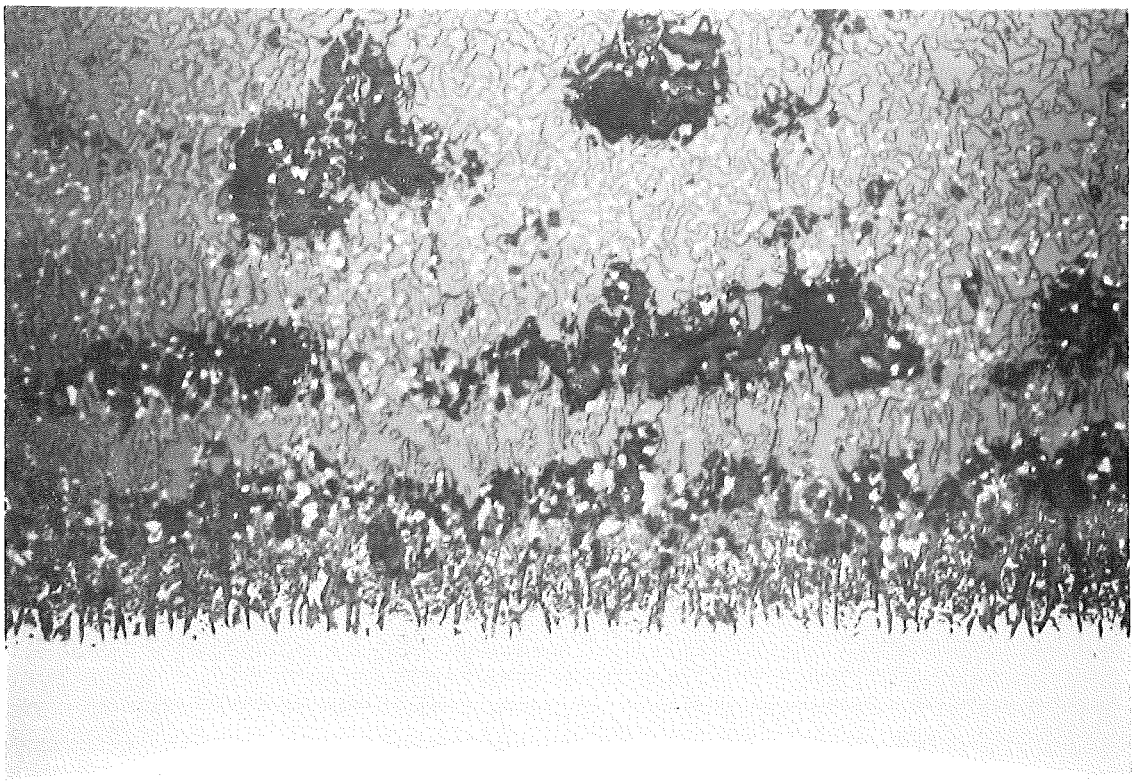

b

Fig. 18. a) Sheet Specimen Oxidized At 1300°C For 5 min
b) Tube Specimen Oxidized At 1300°C For 2,5min
(X500)

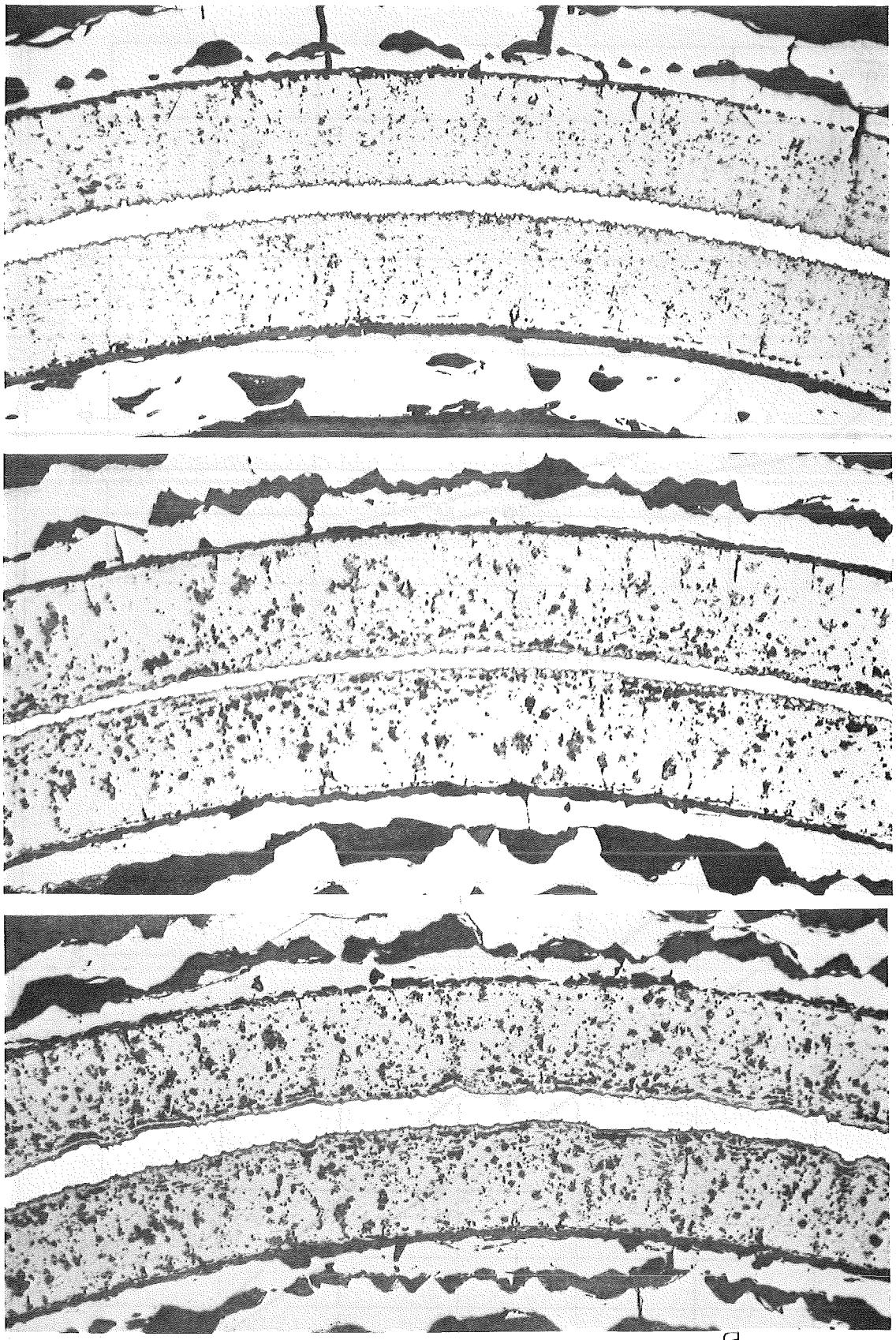

KfK

Fig.19. Tube Specimens Oxidized: a) At 1000°C For 6 h, b) At 1100°C For 1 h, c) At 1200°C For 30 min. (X100)

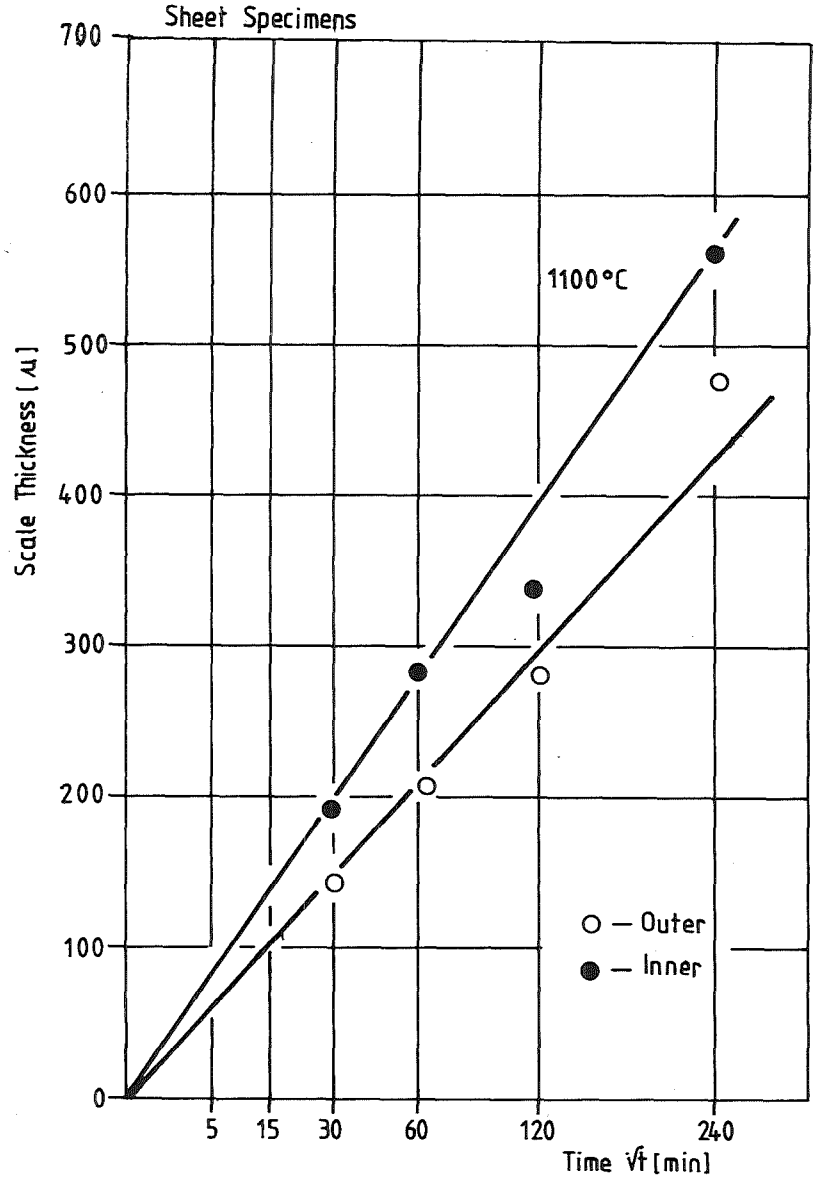

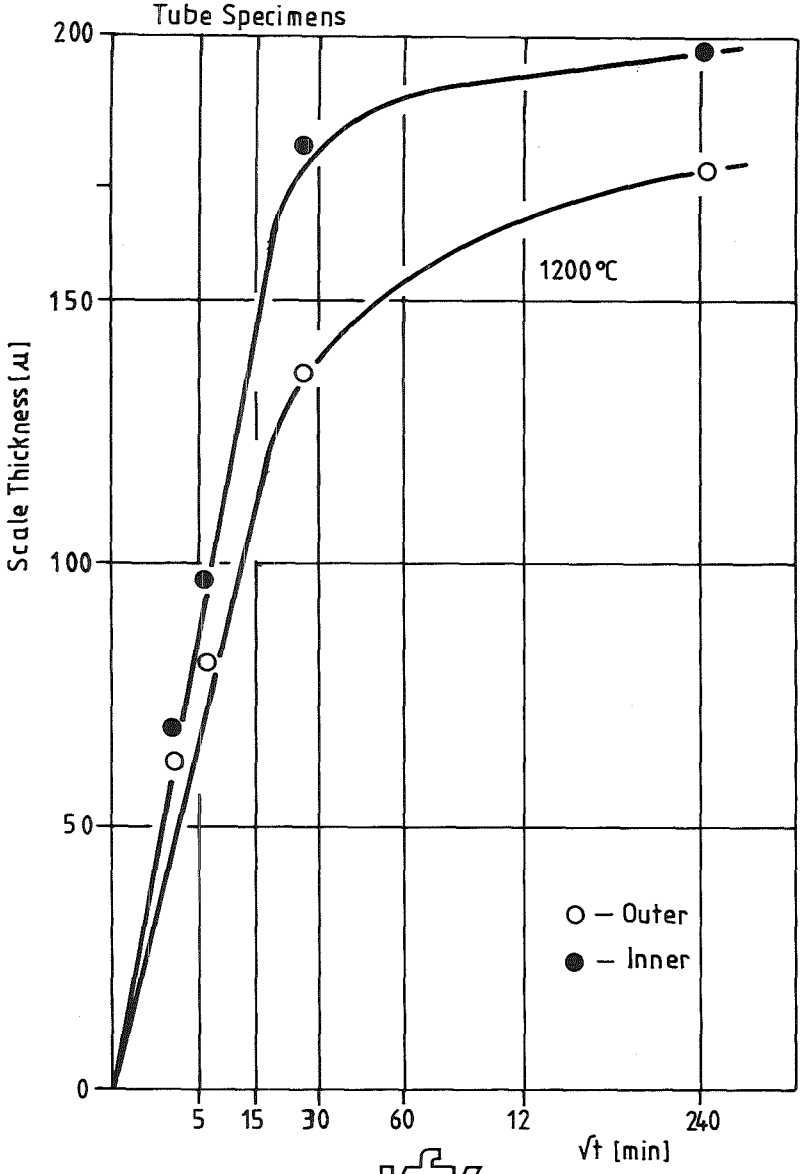

Fig. 20. Thicknesses of the inner and outer layers of scale formed during steam oxidation of ferritic steel No. 1.4914

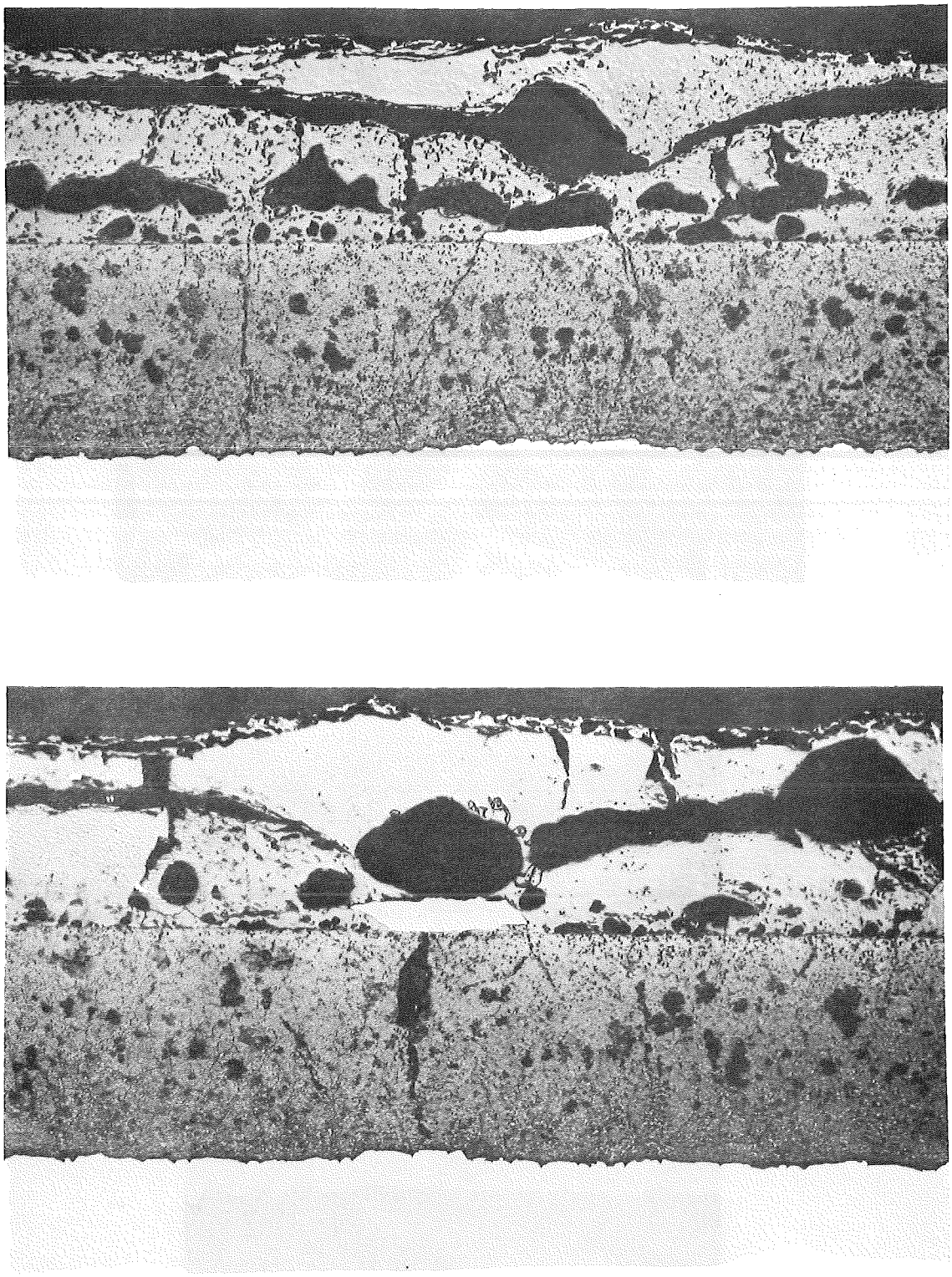

Fig. 21. Photomicrograph Of a Platinum Marker In The Scale Formed On The Sheet Specimen Exposed At 1100°C In Steam (X100)

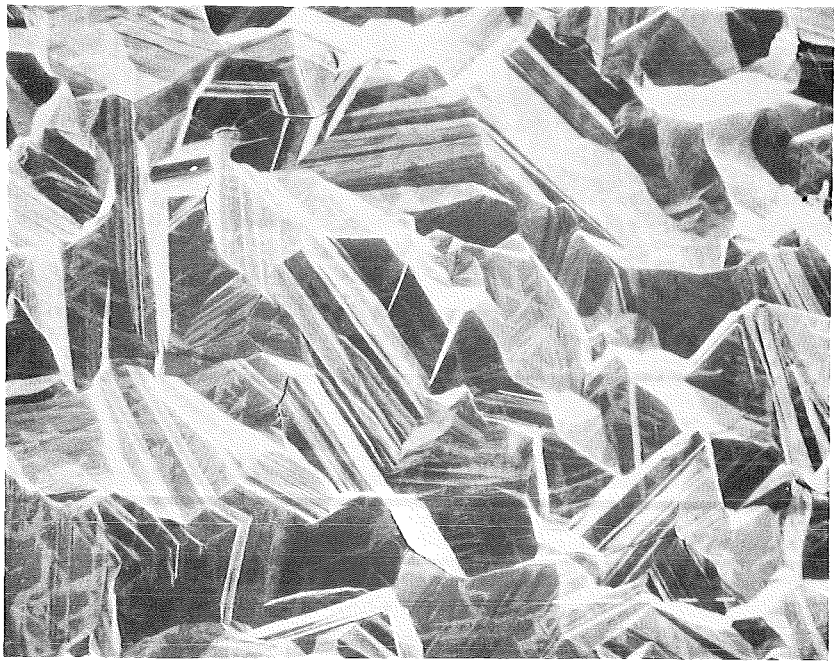

a

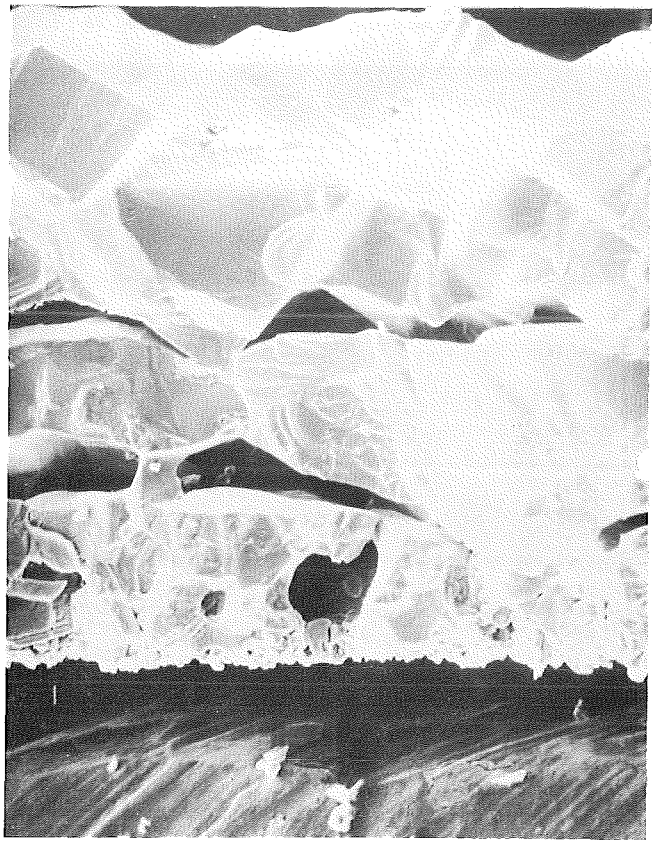

b

Fig. 22. SEM Fractograph of Sheet Specimen Oxidized At 1300 °C For 5 min a) X 100 b) 300